A

Thesis Report

On

"STUDY AND ANALYSIS OF CARRIER FREQUENCY OFFSET (CFO) IN OFDM"

A Thesis Report Submitted in Partial Fulfilment of

Requirement for the Award of Degree of

MASTER OF ENGINEERING

In

Wireless Communication

Submitted By

Nirjan Malla

(Roll No - 801263018)

Under the Guidance of

Dr. Hem Dutt Joshi

Assistant Professor

ECE Department

Thapar University, Patiala

DEPARTMENT OF ELECTRONICS & COMMUNICATION ENGINEERING

THAPAR UNIVERSITY

(Established under section 3 of UGC Act, 1956)

PATIALA - 147004, INDIA

JULY - 2014

DECLARATION

I hereby declare that the work, which is being presented in this thesis, entitled "**STUDY AND ANALYSIS OF CARRIER FREQUENCY OFFSET (CFO) IN OFDM**" in partial fulfilment of the requirements for the award of Master of Engineering in Wireless Communication at Electronics and Communication Engineering Department of Thapar University, Patiala which is an authentic record of my own work carried out under the guidance of **Dr. Hem Dutt Joshi (Assistant Professor)**, Electronics and Communication Department during the fourth semester, 2014.

The matter presented in this thesis has not been submitted in any other University/Institute for the award of Master of Engineering.

Date: 02/07/14

.....

Nirjan Malla

Roll no: 801263018

This is to certify that the above statement made by the student is correct to the best of my knowledge and belief.

Date: 02/07/14

.....

Dr. Hem Dutt Joshi

Supervisor

Countersigned by:

.....

Dr. Sanjay Sharma

Head of Department

ECED, Thapar University, Patiala

.....

Dr. S.K. Mohapatra

Dean of Academic Affairs

Thapar University, Patiala

ACKNOWLEDGEMENT

I would like to give special thanks to my guide **Dr. Hem Dutt Joshi** (Assistant Professor) ECED, Thapar University, Patiala, for his advice, kind assistance, and invaluable guidance. It has been a great honour to work under him.

I am also thankful to **Dr. Sanjay Sharma**, Prof. & Head, Electronics and communication Engineering Department, for providing us with adequate infrastructure in carrying the work.

I am also thankful to **Dr. Kulbir Singh**, P.G. Co-ordinator, Electronics and communication Engineering Department for the motivation and inspiration that triggered me for the report work.

I am greatly indebted to all of my friends who constantly encouraged me and also would like to thank all the faculty members of ECED for the full support of my work. I am also thankful to the authors whose work have been consulted and quoted in this work.

Nirjan Malla

ABSTRACT

A demand for high speed mobile wireless communications is quickly mounting. Wireless communication is the key part of research with growing demand of high data rate applications at a low cost. Orthogonal Frequency Division Multiplexing (OFDM) is a promising answer for this problem. It is a multi-carrier modulation and as well as a multiplexing technique proposed for 3G, 4G, LTE; a systems to support high data rate applications in a fading environment. There are many problems linked with the multi-carrier transmission like phase variations, timing offset, large peak to average power ratio (PAPR), frequency offset etc. in which Carrier Frequency Offset (CFO) is one of the major issues. This frequency offset breaks the orthogonality among the sub-carriers and hence causes inter-carrier interference (ICI) in the OFDM symbol, which seriously degrades the overall system performance.

In this thesis; we have studied and analyzed CFO upon signal to noise ratio (SNR), different techniques to estimate CFO and its effect in detailed for OFDM symbol. The estimation techniques cover both domains; time and frequency for OFDM system. The three types of CFO methods as: CP, Moose, and Classen are compared in MATLAB simulation. In Cyclic Prefix (CP) method, the CFO can be found from the phase angle of the product of CP and corresponding rear part of the OFDM symbol. In CFO estimation using Classen method, the CFO estimation range can be increased by reducing the distance between two blocks of samples for correlation. This was made possible using training symbol that are repetitive with shorter period.

The principles of the eight different methods are reviewed; but among these, three methods has been compared in term of Mean Square Error (MSE) which is verified through MATLAB simulation. From simulation results, the Classen method has best performance and CP method has worst performance because of easy implementation and no loss of bandwidth efficiency. Although, Moose method has similar performance as Classen method in terms of MSE.

CONTENT

CHAPTER 2: OFDM SYSTEM MODEL

CHAPTER 3: LITERATURE SURVEY

CHAPTER 4: RESULTS AND ANALYSIS

CHAPTER 5: CONCLUSION AND FUTURE SCOPE

REFERENCES

LIST OF FIGURES

Figure No Descriptions Page No

LIST OF TABLES

Table No Description Page No

LIST OF ABBREVIATIONS

S. No.	Abbreviation	Description
1	4G	Fourth Generation
2	ACI	Adjacent Channel Interfernce
3	ADSL	Asymmetric Digital Subscriber Lines
4	AWGN	Additive White Gaussian Noise
5	BS	Base Station
6	BLUE	Best Linear Unbiased Estimator
7	CDMA	Code Division Multiple Access
8	CFO	Carrier Frequency Offset
9	CP	Cyclic Prefix
10	DAB	Digital Audio Broadcasting
11	DFT	Discrete Fourier Transform
12	DMT	Discrete Multi-Tone
13	DVB	Digital Video Broadcasting
14	DACE	Data Aided Channel Estimation
15	DDCE	Decision Directed Channel Estimation
16	DSSS	Direct Sequence Spread Spectrum
17	DVB-T	Digital Video Broadcasting Terrestrial
18	CAZAC	Constant Amplitude Zero Autocorrelation
19	FCC	Federal Communications Commission
20	FFO	Fractional Carrier Frequency Offset
21	FFT	Fast Fourier Transform
22	FMT	Filtered Multi-Tone
23	GSTN	General Switched Telephone Network
24	HDSL	High Bit Rate Digital Subcarriers Line
25	HDTV	High Definition Television
26	HYPERLAN	High Performance Radio LAN
27	HDTV-T	High Definition Television Terrestrial
28	ICI	Inter-Carrier Interference
29	IFO	Integer Carrier Frequency Offset
30	ISI	Inter-Symbol Interference

31	IDFT	Inverse Discrete Fourier Transform
32	IEEE	Institute of Electrical and Electronics Engineering
33	IFFT	Inverse Fast Fourier Transform
34	LP	Last Prefix
35	MAC	Medium Access Control
36	MCM	Multi Carrier Modulation
37	ML	Maximum Likelihood
38	MSE	Mean Square Error
39	M-QAM	M-ary Quadrature Amplitude Modulation
40	NLOS	Non Line of Sight
41	OFDM	Orthogonal Frequency Division Multiplexing
42	PLL	Phase Lock Loop
43	PSD	Power Spectral Density
44	PAPR	Peak-to-Average-Power Ratio
45	QAM	Quadrature Amplitude Modulation
46	QPSK	Quadrature Phase Shift Keying
47	SC	Single Carrier
48	S/P	Serial to Parallel converter
49	SNR	Signal to Noise Ratio
50	TS	Terminal Station
51	UHF	Ultra High Frequency
52	VCs	Virtual Carriers
53	VHDSL	Very High Rate Digital Subscriber Line
54	WLL	Wireless Local Loop
55	WLAN	Wireless Local Area Network

CHAPTER 1 INTRODUCTION

1.1 OVERVIEW

Orthogonal frequency division multiplexing (OFDM) is one of those aspects that had been deploying for a long time, and became a practical reality when the presence of mass market applications occur at the same time with the availability of electronic technologies and efficient software. Currently, OFDM stands as the prime technology for 4G [1].

OFDM is a special form of multicarrier modulation process that promises higher performance. OFDM has been taken as the modulation method, since it is the most spectrally efficient method created so far [2]. It mitigates the severe problems related multipath propagation that causes loss of signal in the microwave and UHF spectrum and on data errors. It is been adopted to several wireless local area network (WLAN) standards, as well as asynchronous digital subscriber line (ADSL), digital audio broadcasting (DAB), and digital video broadcasting (DVB) which provides a method of delivering high speed data rate [3].

1.2 HISTORY AND DEVELOPMENT OF OFDM

OFDM had been used by US military in several high frequency military systems such as KINEPLEX, ANDEFT and KATHRYN [1]. OFDM was first launched in January 1958 [4] but was brought into practical in the 1960s. However, when OFDM was first launched, it was not very popular because of the complexity of large arrays of sinusoidal generators, cost, and coherence demodulators. In December 1966, Robert W. Chang [5] outlined a theoretical way to transmit simultaneous data stream through linear band limited channel without inter symbol interference (ISI) and inter carrier interference (ICI). Subsequently, he obtained the first US patent on OFDM in 1970 [6]. A major breakthrough in the history of OFDM came in 1971 when Weinstein and Ebert [7] used discrete Fourier transform (DFT) to perform baseband modulation and demodulation focusing on efficient processing.

OFDM started gaining popularity only when discrete Fourier transform (DFT) and Inverse discrete Fourier transform (IDFT) was made possible without the use of large number of sinusoidal generators. In September 1999 [8], OFDM was accepted as a

wireless local area network (WLAN), but it was not the first IEEE physical standard for WLANs. In June 1997, the first standard was approved and three physical layers (IEEE 802.11 FHSS, IEEE 802.11 DSSS, IEEE 802.11 IR) as well as one medium access control (MAC). The IEEE 802.11 direct sequence spread spectrum (DSSS) supports both 1 Mbps and 2 Mbps where other two supports either 1 or 2 Mbps. In July 1998, a high data rate DSSS (IEEE 802.11b) was used for standardization due to the demand of higher throughput where the data rate is increased up to 11 Mbps. Similarly standards IEEE 802.11a and IEEE 802.11b were developed simultaneously. In January 1997, spectrum of 300 MHz in the 5.2 GHz band was released by the federal communications commission (FCC) for WLAN applications where it was specially designed for IEEE 802.11a to use this spectral band. IEEE 802.11a is considered as physical standard for OFDM and now also called fourth generation mobile communication systems.

1.2.1 Present Status

Due to flexible system architecture, OFDM is being used in a number of wired and wireless data and voice applications. Some examples which are recently deployed applications of OFDM are DAB (digital audio broadcasting), cellular radio, DVB-T (digital video broadcasting Terrestrial), HDSL (High-Rate Digital Subscriber Line), ADSL (Asymmetric Digital Subscriber Line), VHDSL (Very High-Rate Digital Subscriber Line), HDTV-T (High Definition TV-T), IEEE 802.11 and Hiper LAN/2, GSTN (General Switched Telephone Network) [9, 10, and 11].

There are many wireless communication systems and network standards still being developed based on OFDM. Further, this technique will be easily observed as most significant impact on the future wireless networks and digital communications.

1.3 FUNDAMENTALS OF MULTI-PATH FADING CHANNEL

The description of multi-path fading channel is elaborated as follows:

1.3.1 Radio Channels

Mobile radio channels are assigned to be the most difficult channels as they suffer from many imperfections such as shadowing, Doppler shift, interference, and multi-path fading. As shown in Figure 1.3.1.1, the transmitted signal suffers from different effects which are described as:

1.3.1.1 Multi-Path Propagation: occurs only as an effect of reflections, diffraction, and scattering of the transmitted electromagnetic wave at natural and man-made objects. Hence we know waves arrive from different directions with different attenuations, phases, and delays. Therefore, superposition of these waves results in phase and amplitude variation of the received signal.

1.3.1.2 Doppler Spread: occurs due to the moving objects in the mobile radio channel. Time variant multi-path propagation occurs only when there is a change in the phases and amplitudes of the arriving waves. Different wave superposition results even there are a small movement on the order of the wavelength.

1.3.1.3 Shadowing: is caused by the obstruction of the transmitted wave, for examples, walls, trees, buildings, hills, which results in more or less strong attenuation of the signal strength. Compared to fast fading, longer distances have to be covered to change the shadowing constellation radically. The varying signal strength due to shadowing is called slow fading and can be described by a log-normal distribution [12].

1.3.1.4 Path Loss: shows how the mean signal power decays with distance between the transmitter and receiver. In free space, the mean signal power decays decreases with the square of the distance between the base station (BS) and terminal station (TS). Here, often no line of sight (NLOS) exits, in a mobile radio channel.

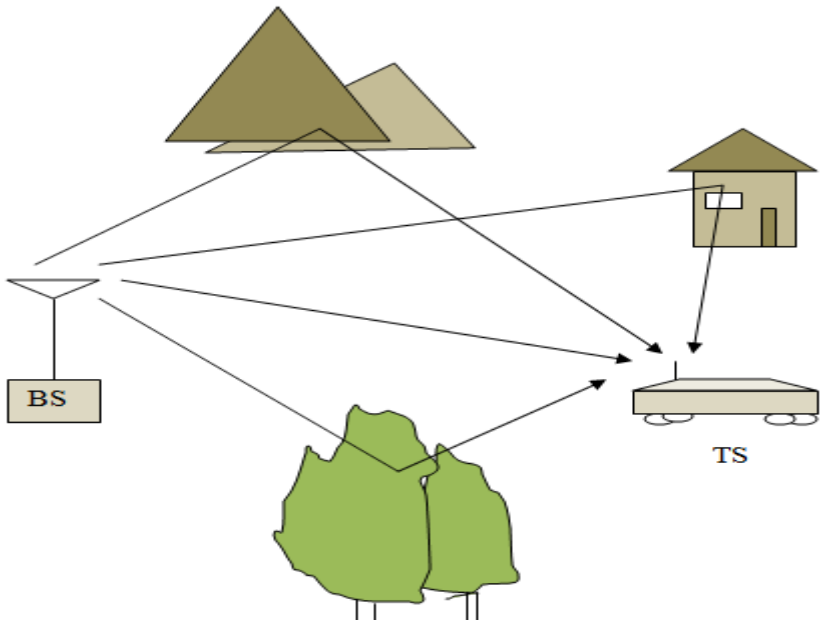

Figure 1.3.1.1 Multi-Path Propagation

1.3.2 Channel Modeling

The mobile radio channel can be characterized by the time-variant channel transfer function $H(f,t)$ or by the time-variant impulse response $h(\tau,t)$. The channel impulse response is composed of a large number of dispersive impulses received over N_p, especially in the environment with multi-path propagation which is given as:

$$h(\tau,t) = \sum_{p=0}^{N_p-1} a_p e^{j(2\pi f_{D,p} t+\varphi_p)}\,\delta(\tau-\tau_p)$$

(1.3.2.1)

where, amplitude $(=a_p)$, Doppler frequency $(=f_{D,p})$, phase $(=\varphi_p)$, and propagation delay $(=\tau_p)$ linked with the path p = 0, ... ,N_p-1.

$$\delta(\tau-\tau_p) = \begin{cases} 1 & if\ \tau=\tau_p \\ 0 & otherwise \end{cases}$$

(1.3.2.2)

Also, the channel transfer functions as:

$$H(f,t) = \sum_{p=0}^{N_p-1} a_p e^{j(2\pi(f_{D,p}\,t-f\tau_p)+\varphi_p)}$$

(1.3.2.3)

The Doppler frequency,

$$f_{D,p} = \frac{v f_c COS(\alpha_p)}{c}$$

(1.3.2.4)

depends on the speed of light $(=c)$, velocity of the terminal $(=v)$, the angle of incidence $(=\alpha_p)$, the carrier frequency $(=f_c)$. The delay power density spectrum $(\rho(\tau))$ gives the average power of the channel output as the function of the delay (τ). The mean delay $(\overline{\tau})$, the root mean square (RMS) delay spread (τ_{RMS}), and the minimum delay $(\tau_{\max})$ are characteristic parameters of the delay power density spectrum. The mean delay is

$$\overline{\tau} = \frac{\sum_{p=0}^{N_p-1} \tau_p \gamma_p}{\sum_{p=0}^{N_p-1} \gamma_p}$$

(1.3.2.5)

where;

$$\gamma_p = \left|\mathrm{a_p}\right|^2$$

(1.3.2.6)

The RMS delay spread is defined as:

$$\tau_{RMS} = \sqrt{\frac{\sum_{p=0}^{N_p-1} \tau_{p^2} \gamma_p}{\sum_{p=0}^{N_p-1} \gamma_p} - \overline{\tau}^2}$$

(1.3.2.7)

The Doppler spread is the bandwidth of the Doppler power density spectrum and can take values up to two times i.e. $f\_Dspread \leq 2|f\_Dmax|$.

1.3 SINGLE-CARRIER VS. MULTI-CARRIER TRANSMISSION

As requirement of a high complexity equalizer to deal with inter-symbol interference problem in a frequency selective or multi-path fading channel causes single-carrier scheme worthless for a high rate wireless transmission. Multi-carrier scheme is worthy for high rate wireless transmission which does not have channel equalization complexity. In a single-carrier transmission, a high data rate may not be feasible due to too much complexity of the equalizer in the receiver.

OFDM and FMT are two different types of multi-carrier scheme. In OFDM, the orthogonality is maintained to each other as well as does not need filter to separate the sub-band and requires a guard band such as Virtual carriers (VCs). In FMT, filter is needed to separate the sub-band but does not need a guard band. There is a case when the number of sub-carriers is less than 64, only in the case of spectral efficiency, FMT is advantageous over OFDM. Other than OFDM and FMT, there are different types of multi-carrier transmission schemes including DWMT (Discrete Wavelet Multi-Tone), OFDM/OQAM-IOTA, and so on [10, 13].

Table 1.3.1 Comparisons between S-C and M-C Transmission Schemes

SINGLE-CARRIER TRANSMISSION		**MULTI-CARRIER TRANSMISSION**	
		OFDM/DMT	**FMT**
Guard Interval	Not required	Required (CP)	Not required
Guard Band	Not required	Required (VC)	Not required
Sub-Carrier Spacing	-	1/(symbol duration)	≥1/(symbol duration)
Pulse Shaping	Nyquist filter (e.g., raised cosine filter)	Window (e.g., rec.)	(e.g., raised cosine)
Sub-Channel Separation	-	Orthogonality	Bandpass filter
Merits	Simple in flat fading	High bandwidth efficiency for large number of sub-carriers (≥64)	Small ACI
Demerits	High complexity equalizer required for frequency selective channel	Low bandwidth efficiency and large ACI for a small number of sub-carriers	High bandwidth efficiency for small number of sub-carriers (<64)

Table 1.3.1 summarizes the differences between the single-carrier and multi-carrier transmission schemes including their advantages and disadvantages.

1.4.1 Multi-Carrier Modulation and Demodulation

The transmitted baseband signal [14] is given by

$$s(t) = \frac{1}{N_c} \sum_{i=-\infty}^{+\infty} \sum_{n=0}^{N_c-1} d_n g(t - iT_s) e^{j2\pi f_n t}$$

(1.4.1.1)

where, number of sub-carriers$(= N_c)$, symbol rate linked with each sub-carrier$(= 1/T_s)$, impulse response of the transmitter filters$\big(= g(t)\big)$, complex symbol $(= d_{n,i})$, and frequency of sub-carrier $(= f_n)$. In Figure 1.4.1.1, after symbol mapping, each block of N_c complex-valued symbols is serial-to-parallel (S/P) converted and then transmitted to multi-carrier modulator where the symbols are transmitted simultaneously on N_c, occupying a small fraction $(\frac{1}{N_c})$ of the total bandwidth *B*.

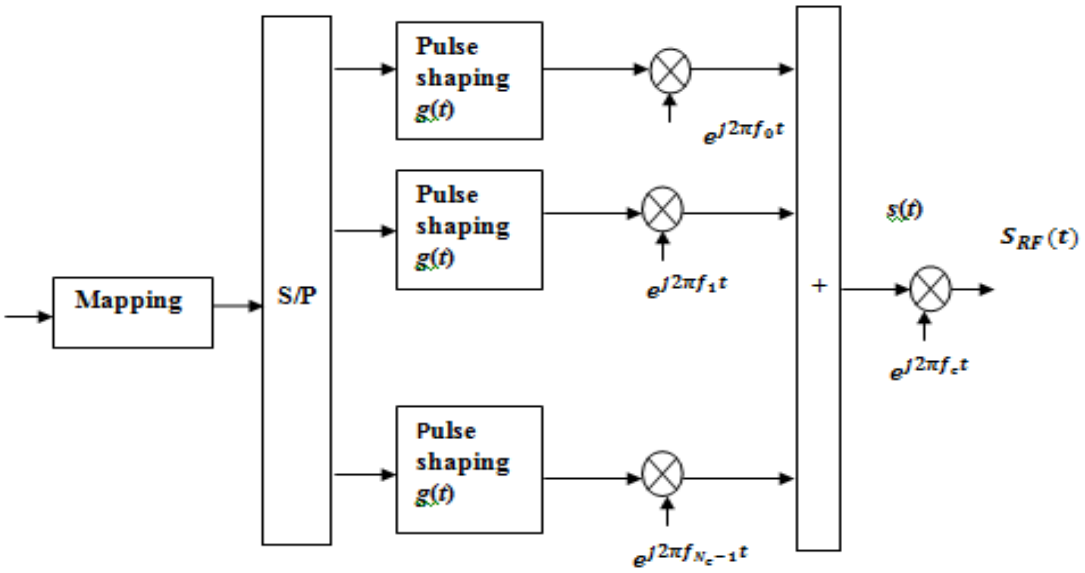

Figure 1.4.1.1 Block Diagram of a Multi-Carrier Transmitter

Now we consider equally spaced sub-carriers as:

$$f_n = \frac{n}{T_s} \qquad n = 0,1,\ldots..N_c - 1$$

(1.4.1.2)

The up-converted transmitted RF signal $S_{RF}(t)$ can be expressed by;

$$S_{RF}(t) = \frac{1}{N_c}\mathrm{Re}\left\{\sum_{i=-\infty}^{+\infty}\sum_{n=0}^{N_c-1} d_{n,i}\, g(t-iT_s)\, e^{j2\pi(f_n+f_c)t}\right\}$$

$$= \mathrm{Re}\{s(t)e^{j2\pi f_c t}\}$$

(1.4.1.3)

where, carrier frequency $(= f_c)$. Now as shown in Figure 1.4.1.2, after the down conversion of the RF signal $r_{RF}(t)$ at the receiver side, all is required is the bank of N_c matched filters to demodulate all sub-carriers. After demodulating and filtering, the received baseband signal before sampling at sub-carrier frequency $(= f_m)$ is given as:

$$r_m(t) = \left[r(t)e^{-j2\pi f_m t}\right] \Theta h(t)$$

$$= \left[\sum_{i=-\infty}^{+\infty}\sum_{n=0}^{N_c-1} d_{n,i}\, g(t-iT_s)\, e^{j2\pi(f_n+f_m)t}\right] \Theta\, h(t)$$

(1.4.1.4)

Here, impulse response of the receiver filter $\left(= h(t)\right)$, convolution operation $(= \Theta)$, and after sampling at $t = lT_s$, the sample results in $r_m(lT_s) = d_{m,l}$, if only both the transmitter and receiver of the system fulfil both the ISI and ICI free Nyquist condition [15].

The employment of a time-limited rectangular pulse shaping in the OFDM leads to a simple digital implementation. The optimum value approaches to 1 bits/Hz for the larger for larger number of sub-carriers. The impulse response of the receiver as:

$$h(t) = \begin{cases} 1 & \text{if } -T_s < t \le 0 \\ 0 & \text{otherwise} \end{cases}$$

(1.4.1.5)

The absence of ICI and ISI is fulfilled from the above condition. In the case of inserting a guard time $(= T_g)$, the OFDM spectral efficiency will be reduced to $1 - T_g/(T_s + T_g)$ for larger number of N_c. To fulfil these conditions, different pulse shaping filtering can be implemented as:

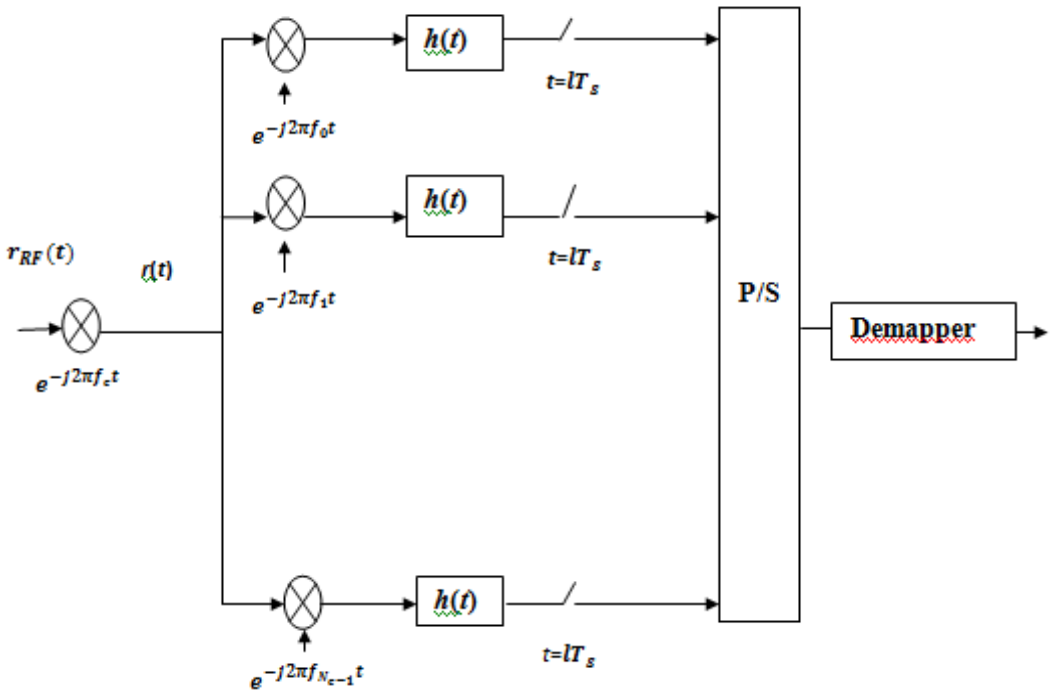

Figure 1.4.1.2 Block Diagram of a Multi-Carrier Receiver

- **Rectangular Band-Limited System**

The impulse response is given to each individual sub-carrier which has rectangular band-limited transmission filter as:

$$g(t) = \frac{\sin\left(\pi \frac{\mathrm{t}}{\mathrm{T_s}}\right)}{\pi \frac{\mathrm{t}}{\mathrm{T_s}}} = \mathrm{sinc}\left(\pi \frac{t}{T_s}\right) \qquad \textbf{(1.4.1.6)}$$

The spectral efficiency of the system equals to the normalized value of 1 bits/Hz or we can say optimum value.

- **Rectangular Time-Limited System**

The impulse response is given to each individual sub-carrier which has rectangular time-limited transmission filter as:

$$g(t) = rect(t) = \begin{cases} 1 & 0 \le t < T_s \\ 0 & \text{otherwise} \end{cases}$$

(1.4.1.7)

The spectral efficiency of the system equals to the normalized values $1/(1 + (BT\_s)/N\_c)$. The optimum value approaches to 1 bits/Hz for the larger N_c.

- **Raised Cosine Filtering**

In [15] each sub-carrier is filtered by a time-limited $(t \in -kT_s^{'}, kT_s^{'}\})$ square root of raised cosine filter with roll-off factor α and impulse response as:

$$g(t) = \frac{\sin\left[\pi \frac{t}{T_s^{'}}(1-\alpha)\right] + \frac{k\alpha t}{T_s^{'}}\cos\left[\pi \frac{t}{T_s^{'}}(1+\alpha)\right]}{\pi \frac{\mathrm{t}}{\mathrm{T_s}}\left[1 - \left(\frac{\mathrm{k\alpha t}}{T_s^{'}}\right)^2\right]}$$

(1.4.1.8)

Here, $T_s^{'} = (1+\alpha)\mathrm{T_s}$ and k is the maximum number of samples that the pulse shall not exceed. The spectral efficiency of the system equals to the normalized values $1/(1 + (1+\alpha)/N\_c)$. The optimum value approaches to 1 bits/Hz for the larger N_c.

1.5 PRINCIPLE OF OFDM

The basic principle of OFDM is to split a high rate data streams into number of lower rate data streams that are transmitted simultaneously over a number of sub-carriers. The comparative amount of dispersal in time caused by multipath delay spread is decreased, as the symbol duration increases for lower rate parallel sub-carriers. In OFDM, such as number of subcarriers, symbol duration, guard time, modulation type per sub-carriers, and sub-carrier spacing are the different parameters set up for consideration. The system requirements such as Doppler values, available bandwidth, tolerable delay spread, and required bit rate are influenced by the choice of parameters.

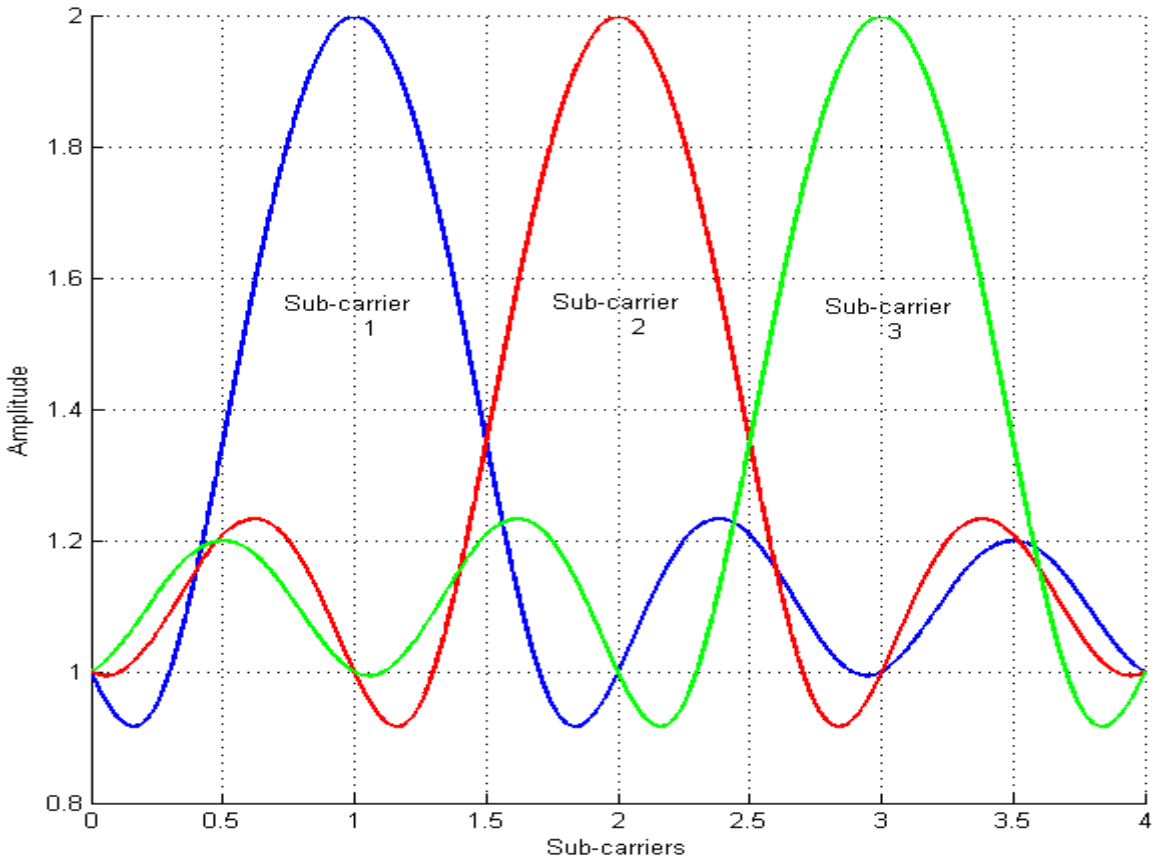

Figure 1.5.1 Orthogonality among three Sub-Carriers

Consider the time limited complex exponential signal $\{e^{j2\pi tf_k}\}_{k=0}^{N-1}$ which represents the different subcarriers at $f_k = k/T_{sym}$ in the OFDM signal, where $0 \leq t \leq$ T_sym. These signals are defined to be orthogonal if the integral of the products for the common period is nil, so as to is,

$$\frac{1}{T_{sym}}\int_0^{T_{sym}} e^{j2\pi tf_k}\, e^{-j2\pi tf_i}\, dt = \frac{1}{T_{sym}}\int_0^{T_{sym}} e^{j2\pi t\frac{k}{T_{sym}}}\, e^{-j2\pi t\frac{i}{T_{sym}}}\, dt$$

$$= \frac{1}{T_{sym}}\int_0^{T_{sym}} e^{j2\pi\frac{k-i}{T_{sym}}t}\, dt$$

$$= \begin{cases} 1, & \forall \text{ integer } k = i \\ 0, & \text{otherwise} \end{cases}$$

(1.5.1)

The above orthogonality is a condition for an OFDM signal. Normally, in OFDM, spectrally overlapped sub-carriers can be used as they are orthogonal, they do not

superposed with one other which in turn causes OFDM a bandwidth efficient modulation scheme. Orthogonality of sub-carriers must be guaranteed to avoid ICI.

1.5.1 OFDM Transmission Scheme [16]

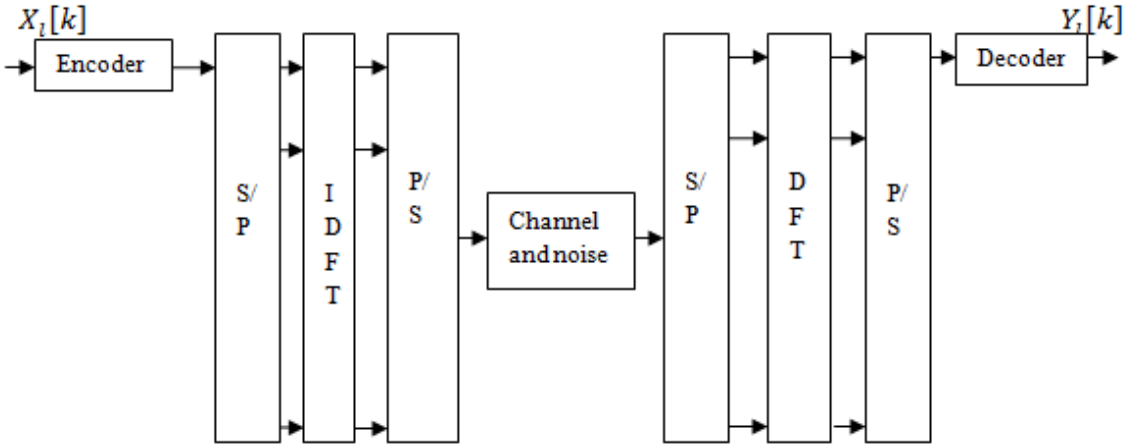

Figure 1.5.1.1 OFDM Transmission Scheme implemented using IDFT/DFT

As shown in Figure 1.5.1.1, it does not use individual oscillator and bandlimited filter for each sub-channel and for bandwidth efficiency; the spectrum of sub-carriers are overlap. In implementing these orthogonal signals, discrete Fourier transform (DFT) and inverse DFT (IDFT) are useful. But now DFT and IDFT can be effectively implemented using fast Fourier transform (FFT) and inverse FFT (IFFT) respectively. In this system, consider N-point IFFT as transmitted symbols $\{X_l[k]\}_{k=0}^{N-1}$, so as to producing $\{x[n]\}_{n=0}^{N-1}$, the samples as a sum of N orthogonal subcarriers signal. Now received sample as $y[n]$ correspond to $x[n]$ with addition of noise $w[n]$ i.e. can say $y[n] = x[n] + w[n]$. Now taking received samples for N-point FFT, $\{y[n]\}_{n=0}^{N-1}$, the noisy version of the transmitted symbols $\{Y_l[k]\}_{k=0}^{N-1}$ can be obtained at the receiver side.

1.6 ADVANTAGES OF OFDM SYSTEMS

1.6.1 Immunity to Delay Spread

The presence of multipath channel is the major problem in most wireless systems. The transmitted signal reflects off of several objects in a multipath environment. As a result, delayed versions of the transmitted signal arrive at the receiver. At the receiver side, it get distorted due to multiple version of signal. The occurrences of the maximum time delay

so called delay spread of the signal in that environment. In OFDM, there occur two problems due to multipath channel [17]. The first problem is inter-symbol interference (ISI) which occurs when the received OFDM symbol is distorted by the previously transmitted OFDM symbol. In single-carrier system, the effect of ISI is same, but the interference is typically due to several other symbols instead of previous symbol. In single-carrier system, the symbol period is much shorter than the time span of the channel, whereas the typical OFDM, the symbol period is much longer than the time span of the channel. The next trouble is called Intra-symbol interference, which is the outcome of interference among a given OFDM symbol's own sub-carriers.

The use of discrete- time property is the solution to the problem of intra-symbol interference. It is not practical to have an infinite length OFDM symbol; however, it is possible to make the OFDM symbol as periodic. This periodic form is achieved by replacing the guard interval with a cyclic prefix of length LP sample. The cyclic prefix is a copy of the last LP samples of the OFDM symbol where LP>CP. The cyclic prefix is discarded at the receiver because it contains redundant information. Similar in the case of the guard interval, the effect of inter-symbol is removed using these steps.

1.6.2 Simple Equalization

In OFDM, the time-domain signal is still convolved with the channel response. However, in the receiver side by the help of FFT, the date will be transformed back into frequency-domain. This time-domain convolution will result in the multiplication of the spectrum of the OFDM signal with the frequency response of the channel because of the periodic nature of cyclically-extended OFDM symbols. The result is each subcarrier's symbol will be multiplied by complex number which equal to channel frequency response at that sub-carrier's frequency. Due to the channel, each received sub-carrier experiences amplitude and phase distortion. To reverse these effects, a frequency-domain equalizer consists of a simple complex multiplication for each subcarrier is employed which is much simpler than a time-domain equalizer.

1.6.3 Efficient Bandwidth Usage

In OFDM, the main concept is orthogonality of sub-carriers. We know area under one period of a sine or a cosine wave is zero, as the carriers are all sine/cosine wave. Each

sub-carriers has a different frequency and it is chosen in such a way that the integral number of cycles in a symbol period signal are mathematically orthogonal.

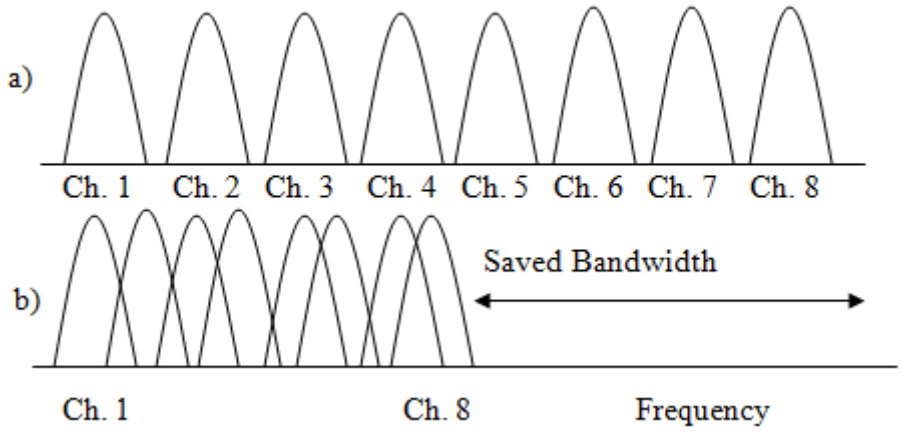

Figure 1.6.3.1 Bandwidth Saving in OFDM

1.6.4 Resistance to Frequency Selective Fading

In the case of single carrier modulation techniques, the complex equalization is required if the channel undergoes frequency selective fading but in the case of OFDM the available bandwidth is split among many orthogonal narrowly spaced sub-carriers. We can say that if the channel gain/phase associated with the sub-carriers vary, then the sub-carrier experiences flat fading. Even if some sub-carrier are lost completely due to fading, then we can recover user data by applying proper coding and inter-leaver at the transmitter.

1.7 LIMITATIONS OF OFDM SYSTEM

1.7.1 Large Peak to Average Power Ratio (PAPR)

PAPR is proportional to the number of sub-carriers used for OFDM systems. An OFDM system with huge number of sub-carriers will thus have a very large PAPR when the sub-carriers add up logically. Large PAPR of a system makes the execution of DAC and ADC to be tremendously hard. The devise of RF amplifier also becomes increasingly difficult as the PAPR increases.

1.7.2 Synchronization Issues

Demodulation of an OFDM signal with an offset in the frequency can lead to a high bit error rate. The source of synchronization errors are two; first one being the difference

between local oscillator frequencies in transmitter and receiver, secondly relative motion linking the transmitter and receiver that gives Doppler spread. Local oscillator frequencies at mutually points must match as closely as they can. For higher number of sub-channels, the matching should be even more perfect. Motion of transmitter and receiver causes the other frequency error. So, OFDM may show significant performance degradation at high-speed moving vehicles [18]. To optimize the performance of an OFDM link, accurate synchronization is a prime importance. Synchronization needs to be done in three factors: symbol, carrier frequency and sampling frequency synchronization.

1.8 APPLICATIONS AND STANDARDS

In Mobile and Fixed Wireless Systems; OFDM has been adopted in IEEE 802.16 standards to support peak data rate up to 75Mb/s at the frequency bands at 11 GHz [19]. According to bandwidth of the system, OFDMA in IEEE 802.16-2004 [18] fixes the size of the FFT as 256 and also vary sub-channel space but in the case of IEEE 802.16e-2005 [20], sub-carrier space ($\Delta f = 10.94$ KHz) is maintain same but we can notice the changes in the size of the FFT. In both OFDM and OFDMA the ratio of the length of the CP to the symbol duration may be 1/4, 1/8, 1/16, or 1/32, and the modulation scheme may be QPSK, 16QAM, or 64QAM depending on the channel environment and data rate.

Table 1.8.1 IEEE 802.16-2004

PARAMETERS	**SPECIFICATIONS**			
Bandwidth, B_W, (MHz)	1.75	3.5	5.5	7
Sub-channel space, Δf, (KHz)	7.81	16.6	25.0	31.3
Symbol duration,T_s, (μsec)	128	64	40	32
Sampling frequency,f_s,(MHz)	2	4	6.32	8
FFT size, M	256	256	256	256

Table 1.8.2 IEEE 802.16e-2005

PARAMETERS	SPECIFICATIONS			
Bandwidth, B_W, (MHz)	1.75	3.5	5.5	7
Sub-channel space, Δf, (KHz)	10.9	10.9	10.9	10.9
Symbol duration,T_s, (μsec)	91.4	91.4	91.4	91.4
Sampling frequency, f_s, (MHz)	1.40	5.60	11.2	22.4
FFT size, M	128	512	1024	2048

The key parameters of various multi-carrier based communications standards for WLL [14], WLAN [14], and broadcasting (DAB and DVB) [14], are summarized from Table 1.8.3 to 1.8.5.

Table 1.8.3 WLL Standards

PARAMETERS	IEEE 802.16d, ETSI HIPERMAN	
Bandwidth	From 1.5 to 28 MHz	
Number of sub-carriers N_c	256 (OFDM mode)	2048 (OFDMA mode)
Symbol duration T_s	From 8 to 125 μs (depending on bandwidth)	From 64 to 1024 μs (depending on BW)
Guard time T_g	From 1/32 up to 1/4 of T_s	
Modulation	QPSK, 16-QAM, 64-QAM	
FEC Coding	Reed Solomon + Convolutional with code rate 1/2 up to 5/6	
Maximum data rate	Up to 26 Mbit/s	

Table 1.8.4 WLAN Standards

PARAMETERS	VALUES
Number of Data Sub-carriers	48
Number of Pilot Sub-carriers	4
Total Number of Sub-carriers	52
Sub-carrier Frequency Spacing	0.3125 MHz
IFFT/FFT Period	3.2μs (1/Δf)
Preamble Duration	16 μs
Cyclic prefix (CP) Duration	0.8 μs ($T_{FFT}/4$)
Signal Duration BPSK-OFDM Symbol	4 μs($T_{FFT} + T_{CP}$)
Training Symbol CP Duration	1.6 μs($T_{FFT}/2$)
Symbol Interval	4 μs($T_{FFT} + T_{CP}$)
Short Training Sequence Duration	8 μs($10T_{FFT}/4$)

Table 1.8.5 Broadcasting Standards DAB and DVB-T

PARAMETERS	DAB			DVB-T	
Bandwidth	1.5 MHz			8MHz	
Number of sub-carriers N_c	192 (256FFT)	384(512) FFT	1536 (2kFFT)	1705 (2k FFT)	6817 (8kFFT)
Symbol duration T_s	125μs	250 μs	1ms	224 μs	896 μs
Carrier frequency F_s	8 kHz	4 kHz	1 kHz	4.464 kHz	1.116 kHz
Guard time T_g	31 μs	62 μs	246 μs	$\frac{T_s}{32}, \frac{T_s}{16}, \frac{T_s}{8}, \frac{T_s}{4}$	
Modulation	D-QPSK			QPSK,16-QAM,64-QAM	
FEC Coding	Convolution with code rate 1/3 up to 3/4.			Reed Solomon + convolution with code rate 1/2 up to 7/8.	
Maximum data rate	1.7 Mbit/s			31.7 Mbit/s	

1.9 CHAPTER ORGANIZATION

The dissertation is divided into five chapters. The layouts for these chapters are as follows:

Chapter 1 provides a history and development of OFDM system in wireless communication, fundamentals of multi-path fading channel, single-carrier versus multi-carrier transmission along with modulation and demodulation techniques, details study of the principles of OFDM systems along with OFDM transmission scheme, advantages and disadvantages of using OFDM for communication systems, and its applications.

Chapter 2 describes the basic system model of baseband OFDM including transmitter, channel, and receiver model with the expression of transmitted and received OFDM signal. Also includes, synchronization issues, effects of frequency synchronization errors

in OFDM system, the effect of CFO on degradation of OFDM systems, the relationship between frequency offset and SNR, and details mathematical analysis of frequency offset.

Chapter 3 covers details study for the estimation techniques for CFO, and review of eight different algorithms for estimating CFO are then presented.

Chapter 4 includes the result and analysis for the CFO estimation of three different techniques compared with CP, Moose, and Pilot methods in term of MSE versus SNR with the MATLAB simulation.

Chapter 5 covers the work that has been done on this thesis and the work that can be done in this field in the future followed by references.

The most appealing feature of OFDM is the simplicity of the receiver design due to the efficiency with which OFDM can handle with the effects of frequency-selective multipath channels. Multicarrier systems such as OFDM are, however, more sensitive to carrier frequency offset (CFO) than are single-carrier systems. Here, we have studied the details of OFDM communications systems model and then address the issues related to synchronization, and finally analyzed the frequency offset mathematically.

2.1 OFDM SYSTEM MODEL

In Figure 2.1.1, the discrete time baseband OFDM system model [21] with N sub-carriers consisting of transmitter, channel, and receiver blocks are described below:

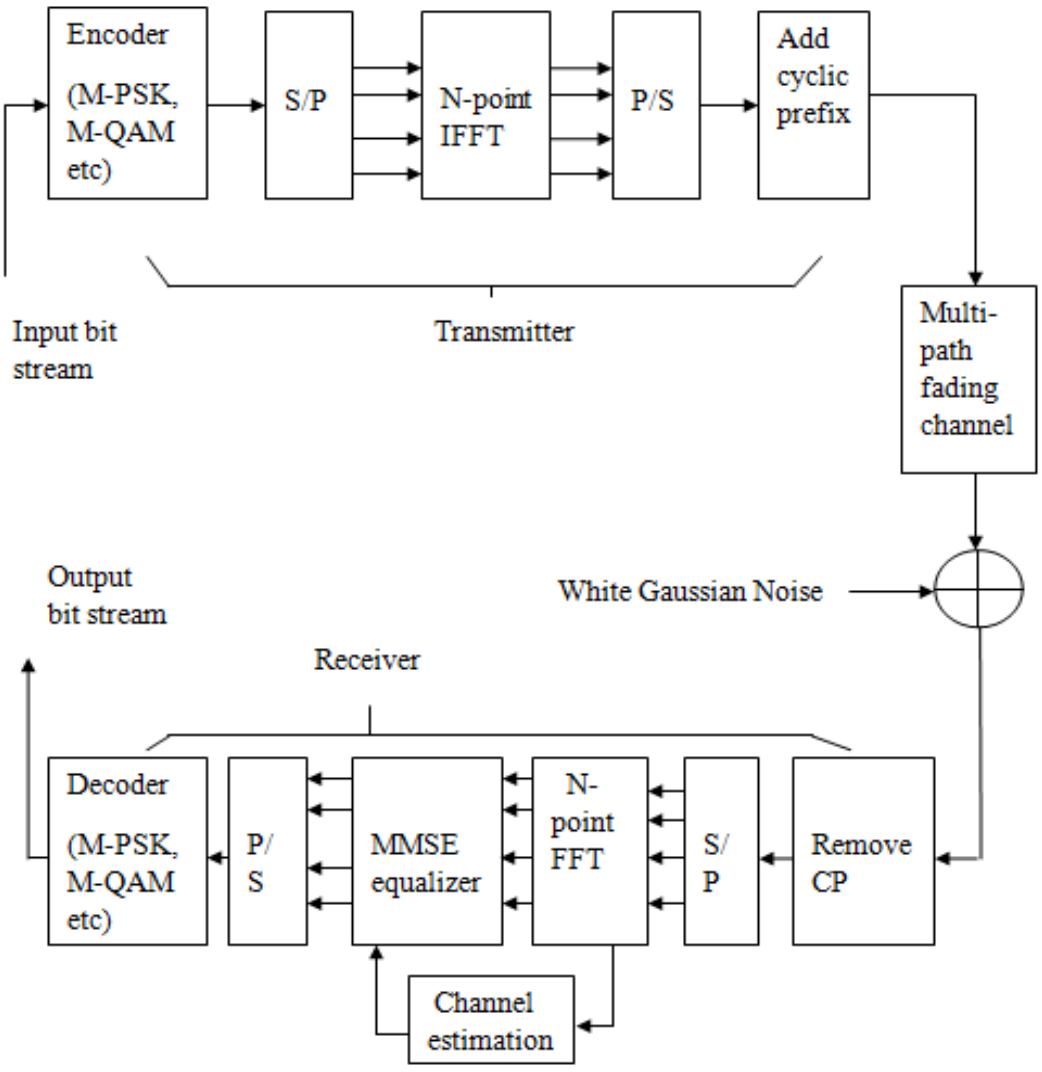

Figure 2.1.1 Baseband OFDM System

2.1.1 OFDM Signal Generation

In the transmitter side as shown in Figure 2.1.1, a block of '***N***' complex data symbols $\{X(k), for\ k = 0,1,2, \dots \dots, N-1\}$ are first transformed from serial to parallel. By utilizing the modulation techniques like M-PSK, M-QAM, etc, the complex data symbols are obtained through encoding $\mathbf{log_2}(\boldsymbol{M})$ inputs. These complex parallel data symbols are then modulated by the group of orthogonal sub-carriers, which satisfy the following orthogonality condition [1].

$$\frac{1}{T_u}\int_0^{T_u} e^{j2\pi f_k t}\, e^{j2\pi f_m t} dt = \begin{cases} 1, k = m \\ 0, k \neq m \end{cases}$$

(2.1.1.1)

where, $f_k = \frac{k}{T_u}, for\ k = 0,1,2, \dots \dots, N-1$ and $\frac{1}{T_u}$is the minimum sub-carrier spacing required. During i^{th} block, the baseband OFDM signal transmission can be as [1].

$$x(i,t) = \frac{1}{N}\sum_{k=0}^{N-1} X(i,k) e^{j2\pi f_k t}, \qquad for\ 0 \leq t \leq T_u$$

(2.1.1.2)

where, $T_u = NT_s$ is the duration of one OFDM symbol, T_s is the sampling interval, $X(i,k)$ is the complex data symbol of i^{th} block, $f\_k = k/T\_u$ is the sub-carrier frequency of k^{th} sub-carrier, N is the total number of sub-carriers. It is considered that compex data symbols are uncorrelated which is as:

$$E[X(i,k)X^*(i,m)] = \begin{cases} 1, k = m \\ 0, k \neq m \end{cases}$$

(2.1.1.3)

Here, $X^*(i,m)$ represents the complex conjugate of $X(i,m)$. The baseband OFDM signal $x(i,n)$ in discrete can be expressed as:

$$x(i,n) = \frac{1}{N}\sum_{k=0}^{N-1} X(i,k) e^{\frac{j2\pi kn}{N}}, \qquad for\ n = 0,1,2, \dots . N-1$$

(2.1.1.4)

From Equation 2.1.1.4, it is clear that the transmitted signal is the inverse discrete Fourier transform (IDFT) of the complex data symbol $X(i,k)$.

2.1.2 Cyclic Prefix or Guard Band Insertion

To avoid the inter-symbol interference (ISI) caused due to the delay spread of multi-path channel, we introduce a guard band interval which is usually inserted between two successive OFDM symbols. Although ISI can be eliminated completely by inserting a guard band interval with no signal transmission but there will be a change in the waveform which contains higher spectral components, so they result in ICI. Hence, the guard interval insertion technique with cyclic prefix (CP) is generally used to avoid ICI which was first introduced by Peled and Ruiz in 1980 [22].

A cyclic prefix (CP) or technique of cyclic extension (CE) was suggested as a solution of maintaining orthogonality, where the OFDM symbol is cyclically extended in the guard time [22].

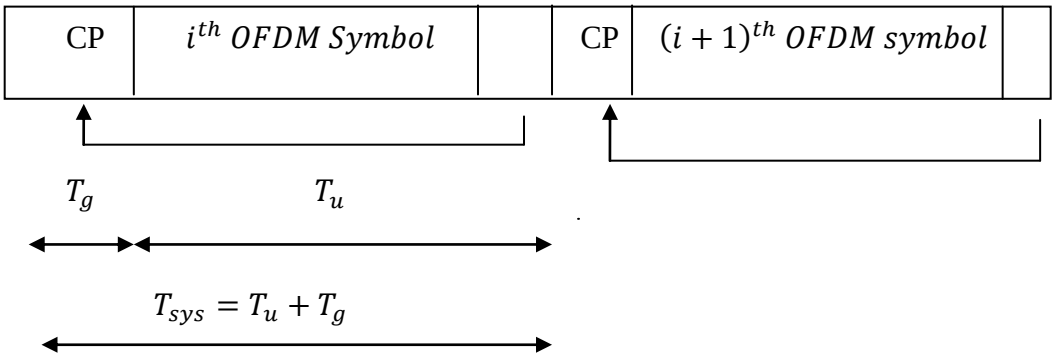

Figure 2.1.2.1 OFDM Symbol with Cyclic Prefix

This above Figure 2.1.2.1 illustrates the insertion of CP. Due to CP insertion; the transmitted signal is extended to $T_{sys} = T_u + T_g$ and can be written as:

$$\tilde{x}(i,t) = \sum_{k=0}^{N-1} X(i,k) e^{j2\pi f_k t} \ , \qquad for \quad -T_g \le t \le T_u \tag{2.1.2.1}$$

where, $\tilde{x}(i,t) = x(i, t+T_u), for -T_g \le t \le 0$. Now baseband OFDM signal with CP is given as:

$$x(i,n) = \begin{cases} x(i,n+N) & for\ \ n = 0,1,2,\ldots..G-1 \\ \frac{1}{N}\sum_{k=0}^{N-1} X(i,k)e^{\frac{j2\pi k(n-G)}{N}}, & for\ n = G, G+1,\ldots..,G+N-1 \end{cases}$$

(2.1.2.2)

where, *N* is total number of sub-carriers and *G* is total number of CP samples appended in the OFDM symbol.

2.1.3 Receiver Model

In the receiver side, the CP is removed only after finding the start of frame and then sample of OFDM symbol is converted from serial to parallel which are then applied to FFT operation. After FFT, channel equalization is performed, and finally applied for decoding process to recover the information symbol. Now received signal is given as:

$$r(i,t) = \sum_{l=0}^{L-1} h_l(\tau)\tilde{x}\,(i, t-\tau_l) + w(i,t)$$

(2.1.3.1)

where, additive white Gaussian noise $(= w(i,t))$. If the length of the CP is greater than the maximum delay spread of the multi-path channel and also if the timing and frequency offsets are correctly estimated and corrected or no offsets, then OFDM signal can be correctly recovered from the received signal. Now after removal of CP, the output of FFT as:

$$\hat{X}(i,k) = H(k)X(i,k) + W(i,k), \qquad for\ \ k = 0,1,2,\ldots\ldots\ldots.N-1$$

(2.1.3.2)

where, frequency response of the multi-path channel $(= H(k))$ and the AWGN component in frequency domain $(= W(k))$. Now the frequency response of channel is given as:

$$H(k) = \sum_{l=0}^{L-1} h_l(\tau)e^{-\frac{j2\pi k\tau_l}{N}}$$

(2.1.3.3)

From Equation 2.1.3.2, the complex data symbol $X(i,k)$ can be recovered by a single complex multiplication of factor $G(k)$, where it is given as:

$$G(k) = \frac{1}{H(K)}$$

(2.1.3.4)

2.1.4 Channel Estimation

Blind and Non-blind are the two types used for the channel estimation for OFDM based system [23, 24, and 25]. The blind channel estimation method uses the large amount of data and the statistical behaviour of the received signals. Due to this, they suffer severe performance degradation in fast fading channels. In the case of non-blind channel estimation method, some part of the transmitted signal are available to the receiver. Furthermore, non-blind channel estimation can be categories into Data Aided channel estimation (DACE) and Decision Directed channel estimation (DDCE).

2.2 SYNCHRONIZATION ISSUES

The message data is being carried out by the OFDM systems on orthogonal sub-carriers for parallel transmission, skirmishing the deformation caused by the frequency selective channel or inter symbol interference in multipath fading channel. If orthogonality is not maintained, its performance may be degraded due to inter symbol interference (ISI) and inter channel interference (ICI) [26].Here we discussed in detail on effect of CFO, and let ε denote the normalized CFO and the received baseband signal under the presence of CFO as:

$$y_l[n] = \text{IDFT}\{Y_l[k]\} = \text{IDFT}\{H_l[k]X_l[k]\} + Z_l[k]$$
$$= \frac{1}{N}\sum_{k=0}^{N-1} H_l[k]X_l[k]e^{\frac{j2\pi(k+\varepsilon)\mathrm{n}}{\mathrm{N}}} + z_l[n]$$

(2.2.1)

where, $z_l[n] = \text{IDFT}\{Z_l[k]\}$

- **Effects of Synchronization Errors**

A large frequency error in the OFDM system causes an increase in ISI and ICI, resulting high degradation in the system performance.

Let us consider the receiver local oscillator frequency$(= f_c)$, and received baseband signal is given as:

$$r(t) = s(t)e^{j2\pi f_{error}t} + n(t)$$

(2.2.2)

where, frequency error $(= f_{error})$, and complex-valued AWGN $(= n(t))$. After filtering and demodulation of the above signal in the absence of fading at sub-carrier ***m*** can be written as [27].

$$r_m(t) = \left[s(t)e^{j2\pi f_{error}t} + n(t)\right]e^{-j2\pi f_m t} \Theta\ h(t)$$
$$= \left[\sum_{i=-\infty}^{+\infty}\sum_{n=0}^{N_c-1} d_{n,i}g(t-iT_s)e^{-j2\pi\left(\frac{n-m}{T_s}\right)t}e^{j2\pi f_{error}t}\right]\Theta\ h(t) + n'(t)$$

(2.2.3)

here, impulse response of the receiver filter $(= n(t))$ and filtered noise $(= n'(t))$. The received signal at the sub-carrier ***m*** is made of four terms as follows:

$$r_m(lT_s + \tau_{error}) = d_{m,l}A_m(\tau_{error})e^{j2\pi f_{error}lT_s} + \mathrm{ISI}_{m,l} + \mathrm{ICI}_{m,l} + n'(lT_s + \tau_{error})$$

(2.2.4)

The second and third term is given as follows:

$$\mathrm{ISI}_{m,l} = \sum_{\substack{i=-\infty \\ i\neq l}}^{+\infty} d_{m,i}\,A_m[(l-i)T_s + \tau_{error}]e^{j2\pi f_{error}iT_s}$$

(2.2.5)

$$\mathrm{ICI}_{m,l} = \sum_{i=-\infty}^{+\infty}\sum_{\substack{n=0 \\ n\neq m}}^{N_c-1} d_{n,i}\,A_n[(l-i)T_s + \tau_{error}]e^{j2\pi f_{error}iT_s}$$

(2.2.6)

$$A_n(t) = \left(g(t)e^{j2\pi f_{error}t}e^{j2\pi\frac{(n-m)t}{T_s}}\right)\Theta\ h(t)$$

(2.2.7)

where, impulse response of the transmitter filter $(= g(t))$, and sample component of Equation 2.2.7 after convolution $(A_n(lT_s))$.

- **Analysis of SNR in Presence of a Frequency Error**

In this section, we concentrate only on effect of frequency error. In above Equation, we substitute $\tau_{error} = 0$ and also we omit guard time for simplicity, then Equation 2.2.6 becomes [27].

$$A_{n(t)} = \begin{cases} e^{j\pi f_{error} t} e^{j\pi \frac{n-m}{T_s} t} \text{sinc}\left[\left(f_{error} + \frac{n-m}{T_s}\right)(T_s - t)\right]\left(1 - \frac{t}{T_s}\right) & ,0 < t \leq T_s \\ 0 & ,otherwise \end{cases}$$

(2.2.8)

After sampling at instant lT_s at sub-carrier $m = n$, $A_m(0) = \text{sinc}(f_{error}T_s)$, and $A_m(lT_s) = 0$. For, $m \neq n$; $A_m(0) = \text{sinc}(f_{error}T_s + n - m)$, and $A_m(lT_s) = 0$. Hence, received data after FFT operation at time $t = 0$ and sub-carrier m can be written as [27].

$$r_m = d_m \,\text{sinc}(f_{error}T_s) e^{j2\pi f_{error}T_s} + \text{ICI}_m + n'$$

(2.2.9)

Here it is obtain by omitting the time index and also we know frequency error does not introduce any ISI. ICI is modelled as AWGN for the large number of sub-carriers. Hence resulting SNR becomes;

$$SNR_{ICI} \approx \frac{|d_m|^2 \text{sinc}^2(f_{error}T_s)}{\sum_{\substack{n=o \\ n \neq m}}^{N_c-1} |d_n|^2 \,\text{sinc}^2(\text{n} - \text{m} + f_{error}T_s) + P_N}$$

(2.2.10)

Here $P_N =$ power of the noise n'. If $\frac{N_0}{2}$ is the noise power spectral density of the AWGN and E_s average received energy of the individual sub-carriers, then;

$$\frac{E_s}{N_0} = \frac{|d_m|^2}{P_N}$$

(2.2.11)

Finally, SNR is given as:

$$SNR_{ICI} \approx \frac{E_s}{N_0} \frac{\text{sinc}^2(f_{error}T_s)}{1 + \frac{E_s}{N_0} \sum_{\substack{n=o \\ n \neq m}}^{N_c-1} \text{sinc}^2(\text{n} - \text{m} + f_{error}T_s)}$$

(2.2.12)

This above Equation 2.2.12 shows that frequency error can cause significant loss in SNR. Furthermore, the SNR depends on the number of sub-carriers.

In Figure 2.2.1, the bound for SNR is tight for lower values of ε and for $\varepsilon = 0.5$. Here, SNR decreases quadratically with the frequency offset or we can say, one can reduce the CP overhead by increasing the number of sub-carriers but this make the system less tolerant to frequency offset.

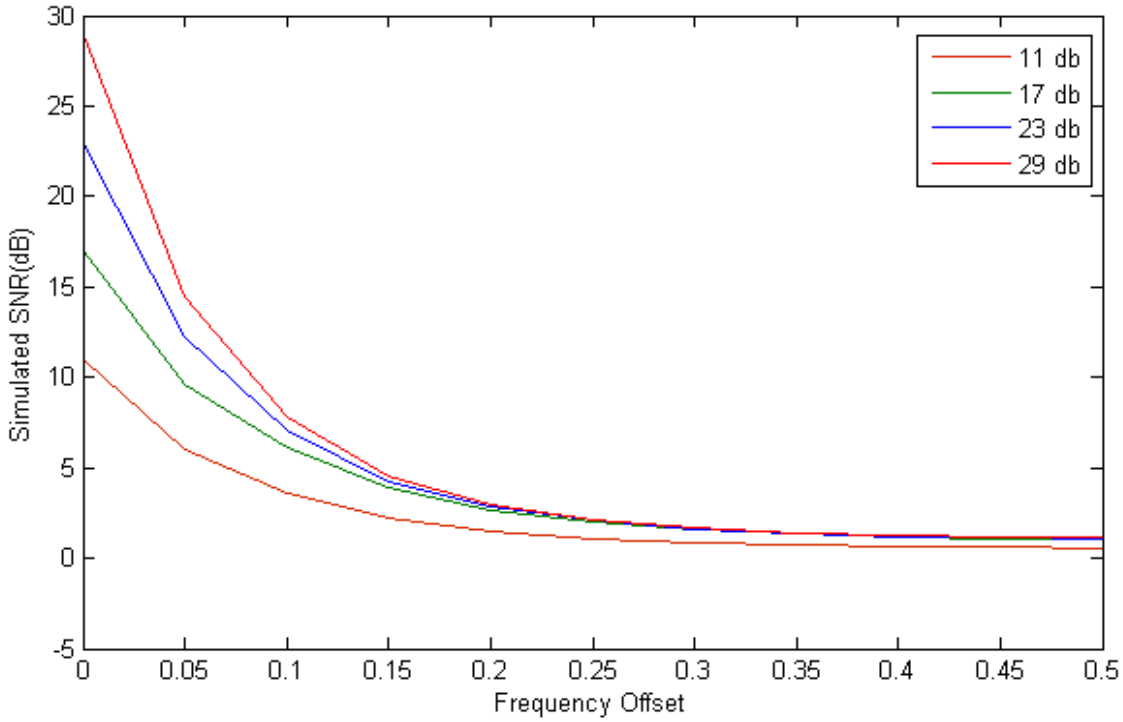

Figure 2.2.1 SNR Vs Frequency Offset

2.3 FREQUENCY SYNCHRONIZATION

Carrier frequency synchronization is one of the fundamental functions of an OFDM receiver. If there is differences in the transmitter and receiver frequencies oscillator, and also due to Doppler shifts and phase noise, there introduces a frequency offset. We recognize frequency offset guide to the demur of signal amplitude since the *sinc* functions are shifted and no longer sampled at the peak and also orthogonality is lost between sub-carrier. Due to this phenomenon there introduces ICI which results in a degradation of whole system performance. Also multi-carrier system is more sensitive to frequency offset than a single-carrier system.

Frequency synchronization can be performed in two steps [14]:

2.3.1 Coarse Frequency Synchronization

Here, consider the frequency offset greater than half of the sub-carrier spacing as:

$$f_{error} = \frac{2z}{T_s} + \frac{\emptyset}{\pi T_s}$$

(2.3.1.1)

Here, first term of above equation represents the frequency offset, which is multiple of sub-carrier spacing where z is an integer and second term is the additional of frequency offset being a fraction of sub-carrier spacing or we can say $\emptyset$ is smaller than π. The main objective of determining the coarse frequency is to estimate z. Different approaches for coarse frequency synchronization can be used depending on the transmitted OFDM signal.

2.3.2 Fine Frequency Synchronization

Under the assumption that frequency offset is less than half of the sub-carrier spacing, there is one to one correspondence between the phase rotation and the frequency offset. The phase ambiguity limits the maximum frequency offset values.

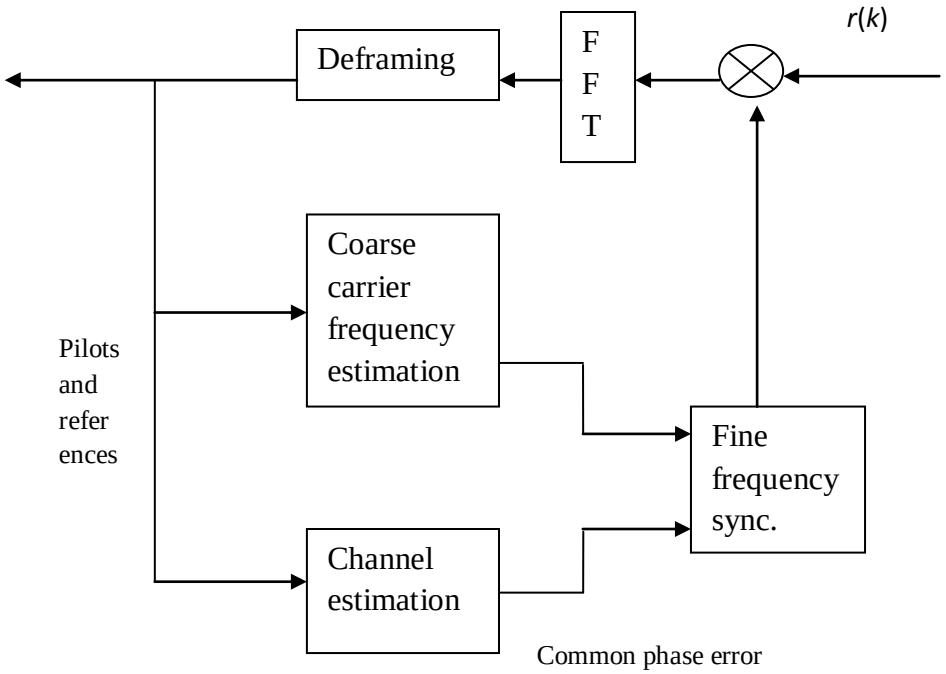

Figure 2.3.2.1 Frequency Synchronization using Reference Symbols

2.4 FREQUENCY OFFSET ANALYSIS

A carrier modulation is used to convert the baseband transmit signal up to the passband and then, by using local carrier signal of the same carrier frequency at the receiver, it is again converted down to the baseband. In general, there are two different type of distortion associated with the carrier signal [28]. The first one is the phase noise caused

due to the instability of carrier signal generators used at the transmitter and receiver. The second one is the carrier frequency offset (CFO) caused by Doppler frequency shift (f_d). Let f_c and $f_c^{'}$ denote the carrier frequencies in the transmitter and receiver respectively. Let their difference be $f_{offset} = f_c - f_c^{'}$; Doppler frequency (f_d) is determined by the carrier frequency (f_c) and velocity (v) of the receiver is $\boldsymbol{f_d} = \frac{\boldsymbol{v.f_c}}{\boldsymbol{C}}$; where, C is the speed of light. Now defining the normalized CFO (ε) as the ratio of the CFO to sub-carrier spacing(Δf) is $\varepsilon = f\_offset/\Delta f$.

Let ε_i and ε_f denotes the integer and fractional part of **ε** respectively, and $\varepsilon = \varepsilon_i + \varepsilon_f$, where $\varepsilon_i = [\varepsilon]$. The effect of CFO (ε) on the received signal $y[n]$ after the transmitted signal $x[n]$ is transmitted [16] is summarized below:

Table 2.4.1 Effect of CFO on the Received Signal

Received Signal		**Effect of CFO on the Received Signal**
Time-domain signal	$y[n]$	$e^{j2\pi n\varepsilon/N}x[n]$
Frequency-domain signal	$Y[k]$	$X[k-\varepsilon]$

To analyse mathematically the effect of carrier frequency offset, the received signal as:

$$r(i,n) = \exp\left(\frac{j2\pi n\varepsilon}{N}\right)\sum_{l=0}^{L-1} h_l(n)\tilde{x}\,(i,n-\tau_l) + w(i,n) \qquad \textbf{(2.4.1)}$$

where, $\varepsilon^{'}$ is the normalized carrier frequency offset by the sub-carrier spacing$\frac{1}{T_u} = \frac{1}{NT_s}$, $h_l(n)$ is the impulse response of the frequency selective multi-path fading channel, τ_l is the path delay of the l^{th} path, and $w(i,n)$ is a zero mean complex value Gaussian noise process with the variance σ_w^2. By assuming a perfect timing synchronization (timing offset $\delta = 0$), the output of FFT can be as:

$$Y(i,p) = \frac{1}{N}\sum_{k=0}^{N-1} X(i,k)H(k)S(k-p+\epsilon) + W(i,p), \quad for\ p = 0,1,2,\ldots\ldots,N-1$$

(2.4.2)

After breaking the summation into two parts:

$$Y(i,p) = \frac{1}{N}X(i,p)H(p)S(\varepsilon) + \frac{1}{N}\sum_{\substack{k=0,\\ k\neq p}}^{N-1} X(i,p)H(k)S(k-p+\varepsilon) + W(i,p), \quad for\ p = 0,1,2,\ldots\ldots,N-1$$

ICI

(2.4.3)

where, $H(k)$ is the frequency response of channel to the sub-carrier k^{th} and $S(k-p+\varepsilon)$ is an ICI co-efficient which is defined as:

$$S(k-p+\varepsilon) = \sum_{n=0}^{N-1} 1 \times e^{\frac{j2\pi n(k-p+\varepsilon)}{N}}$$

$$= e^{j\pi(k-p+\varepsilon)\frac{N-1}{N}} \frac{\sin\left(\pi(k-p+\varepsilon)\right)}{sin\left(\frac{\pi(k-p+\varepsilon)}{N}\right)}$$

(2.4.4)

$$= e^{\frac{j\pi\varepsilon(N-1)}{N}} \frac{\sin(\pi\varepsilon)}{\sin\left(\frac{\pi\varepsilon}{N}\right)} = \begin{cases} N, & for\ \varepsilon = 0 \\ Non-Zero, & for \varepsilon \neq 0 \end{cases}$$

(2.4.5)

The first term in above Equation represents the desired symbol with amplitude distortion due to frequency offset, and second term is ICI , which implies that the orthogonality among sub-carrier frequency components is not maintained any longer due to the frequency offset, and third term is AWGN.

- **Frequency Offset and Inter-carrier Interference**

All OFDM sub-carriers are orthogonal if they all have a different integer number of cycles within the FFT interval. If there is a frequency offset then the number of cycles in the FFT interval is not an integer anymore, as a result ICI occurs after the FFT. The FFT output for each sub-carrier will contain interfering terms from all the other sub-carriers

with an interference power that is inversely proportional to the frequency spacing. The amount of ICI for sub-carriers in the middle of OFDM spectrum is approximately twice as large as that for sub-carriers on both the sides, so there are more interferers within certain frequency distance. The degradation of the SNR $(= D_{freq})$, caused by the frequency offset as:

$$D_{freq} = \frac{10}{3ln10}(\pi \Delta f T)^2 \frac{E_S}{N_0}$$

(2.4.6)

here, frequency offset $(= \Delta f)$, symbol duration in seconds $(= T)$, energy per bit of the OFDM signal $(= E_s)$ and one sided noise power spectrum density (PSD) $(=N_0)$. The frequency offset has an effect like noise and it degrades the SNR, where SNR is the ratio of $\frac{E_S}{N_0}$. From Figure 2.4.1, the SNR degradation increases as the frequency offset increases. Furthermore, CFO causes more degradation to the system operating at high SNR than system operating at low SNR.

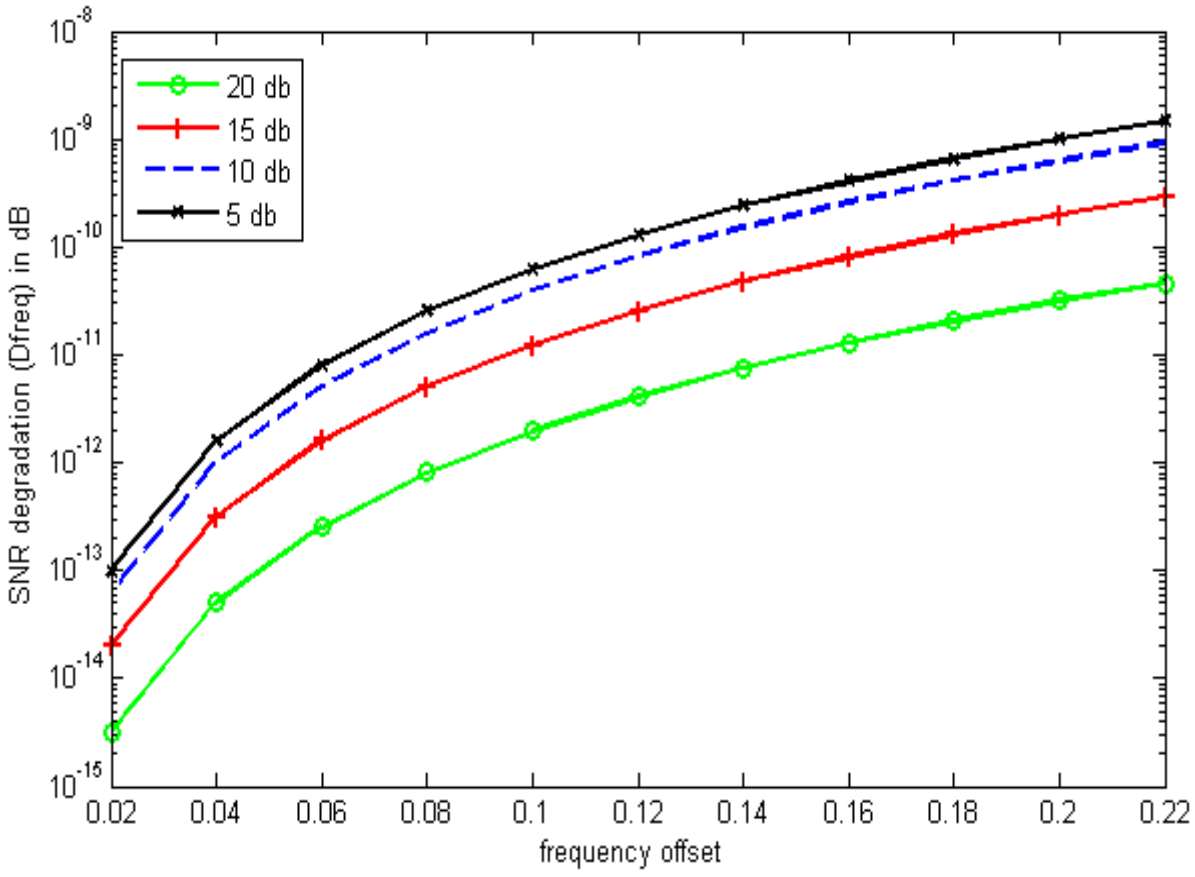

Figure 2.4.1 SNR Degradation Vs Frequency Offset

Further, it is categorized as:

2.4.1 Effect of Integer Carrier Frequency Offset (IFO)

We take a transmit samples as $\{x_l[n]\}_{n=0}^{N-1}$ which experiences a IFO of ε_i .The transmit signal $X[k]$ is cyclically shifted by in the receiver due to the IFO, thus producing $X[k\text{-}\varepsilon_i]$ in the kth sub-carriers. There might causes degradation in the BER performance if unless cyclic shift is adjusted. However, ICI does not occur as well as orthogonality is not destroyed among the sub-carriers frequency components.

2.4.2 Effect of Fractional Carrier Frequency Offset (FFO)

The time domain received signal can be written as:

$$y_l[n] = \frac{1}{N}\sum_{k=0}^{N-1} H(k)X_l[k]e^{\frac{j2\pi(k+\varepsilon)n}{N}} + z_l[n]$$

(2.4.2.1)

Taking the FFT $y_l[n]$, the frequency-domain receives signal with an FFO of ε_f can be written as follows [29]:

$$Y_l[k] = \text{FFT}\{y_l[n]\} = \sum_{n=0}^{N-1} y_l[n]e^{-\frac{j2\pi kn}{N}}$$

(2.4.2.2)

$$= \sum_{n=0}^{N-1}\frac{1}{N}\sum_{m=0}^{N-1} H(m)\,X_l[m]e^{\frac{j2\pi(m+\varepsilon_f)n}{N}}e^{-\frac{j2\pi kn}{N}} + \sum_{n=0}^{N-1} z_l[n]\mathrm{e}^{-\frac{\mathrm{j2\pi kn}}{\mathrm{N}}}$$

(2.4.2.3)

$$= \frac{1}{N}\sum_{m=0}^{N-1} H[m]\,X_l[m]\sum_{n=0}^{N-1} e^{\frac{j2\pi(m-k+\varepsilon_f)n}{N}} + Z_l[k]$$

(2.4.2.4)

$$= \frac{1}{N}H[k]X_l[k]\sum_{n=0}^{N-1} e^{\frac{j2\pi n\varepsilon_f}{N}} + \frac{1}{N}\sum_{m=0,m\neq k}^{N-1} H[m]\,X_l[m]\sum_{n=0}^{N-1} e^{\frac{j2\pi(m-k+\varepsilon_f)n}{N}} + Z_l[k]$$

(2.4.2.5)

$$= \frac{1}{N}\frac{1-e^{j2\pi\varepsilon_f}}{1-e^{\frac{j2\pi\varepsilon_f}{N}}} H[k]X_l[k] + \frac{1}{N}\sum_{m=0,m\neq k}^{N-1} H[m]\,X_l[m]\frac{1-e^{j2\pi(m-k+\varepsilon_f)}}{1-e^{\frac{j2\pi(m-k+\varepsilon_f)}{N}}} + Z_l[k]$$

(2.4.2.6)

$$= e^{\frac{j\pi\varepsilon_f(N-1)}{N}}\left\{\frac{\sin(\pi\varepsilon_f)}{N\sin\left(\pi\varepsilon_{\frac{f}{N}}\right)}\right\}H_l[k]X_l[k] + e^{\frac{j\pi\varepsilon_f(N-1)}{N}}\sum_{m=0,m\neq k}^{N-1}\frac{\sin(\pi(m-k+\varepsilon_f))}{N\sin(\pi(m-k+\varepsilon_f)/N)} H[m]X_l[m]e^{\frac{j\pi(m-k)(N-1)}{N}} + Z_l[k]$$

(2.4.2.7)

$$= \frac{sin\pi\varepsilon_f}{Nsin\pi(\varepsilon_{f/N})}.e^{\frac{j\pi\varepsilon_f(N-1)}{N}} H_l[k]X_l[k] + I_l[k] + Z_l[k]$$

(2.4.2.8)

where,

$$I_l[k] = e^{\frac{j\pi\varepsilon_f(N-1)}{N}}\sum_{m=0,m\neq k}^{N-1}\frac{\sin(\pi(m-k+\varepsilon_f))}{N\sin(\pi(m-k+\varepsilon_f)/N)} H[m]X_l[m]e^{\frac{j\pi(m-k)(N-1)}{N}}$$

(2.4.2.9)

The first term of the last line in Equation 2.4.2.8 represents the amplitude and phase distortion of the k^{th} sub-carrier frequency component due to the FFO. Meanwhile, $I_l[k]$ in Equation 2.4.2.8 represents the ICI from other sub-carriers into k^{th} sub-carriers frequency component, which imply that the orthogonality among sub-carrier frequency components is not maintained any longer due to the FFO.

CHAPTER 3 LITERATURE SURVEY

Literature survey of any research field is must required, before contributing in the research of that field. The literature review gives the detailed study of existing published paper for clear understanding of the particular area. Therefore, this chapter provides details about the CFO estimation techniques on time and frequency-domain estimators and detailed literature survey of the area taken related to Carrier Frequency Offset in OFDM.

3.1 CFO ESTIMATION TECHNIQUES

It is essential to estimate the CFO, which explains distortion in the transmitted symbols and hence at the receiver it can be compensated using some of the techniques.CFO estimation can either be performed in the time or the frequency domain. Now, both will be discussed separately.

3.1.1 Time-Domain Estimation

Training symbol or cyclic prefix (CP) is used to estimate the CFO in time-domain. Each of them is described individually.

- **CFO Estimation Techniques using CP**

CFO (ε) with a perfect symbol synchronization results in a phase rotation of $\frac{2\pi n\varepsilon}{N}$ in the received signal. When consider under negligible channel effect, the phase difference between the *N* samples apart spaced of an OFDM symbols and CP caused by CFO (ε) becomes $\frac{2\pi N\varepsilon}{N} = 2\pi\varepsilon$. CFO can be obtained from the phase angle which is the product of the *N* samples apart spaced of an OFDM symbols and CP.

$$\hat{\varepsilon} = \frac{1}{2\pi}\arg\{y_l^*[n]y_l[n+N]\} \qquad n = -1, -2, \ldots\ldots\ldots, -N_g. \tag{3.1.1.1}$$

Now, its average can be taken over the samples in the CP interval in order to reduce noise effect;

$$\hat{\varepsilon} = \frac{1}{2\pi}\arg\left\{\sum_{n=-N_G}^{-1} y_l^*[n]y_l[n+N]\right\}$$

(3.1.1.2)

In Equation 3.1.1.2, arg( ) is performed by using $\tan^{-1}(\,)$, as the CFO acquisition range is [-π, +π)/2π = [-0.5, +0.5), i.e. $|\hat{\varepsilon}| < 0.5$. When there is no frequency offset $y_l^*[n]y_l[n+N]$ becomes real but in fact we can estimate CFO [26] for imaginary part of $y_l^*[n]y_l[n+N][10]$. In this case, the estimation error is defined as:

$$e_\varepsilon = \frac{1}{L}\sum_{n=1}^{L} Im\{y_l^*[n]y_l[n+N]\}$$

(3.1.1.3)

Here, L is the number of samples used for averaging. The expectation of error function (e_ε) can be approximated as:

$$E\{e_\varepsilon\} = \frac{\sigma_d^2}{N}\sin\left(\frac{2\pi\varepsilon}{N}\right)\sum_{k\ corresponding\ to\ useful\ carriers}^{L} |H_k|^2 \approx K_\varepsilon$$

(3.1.1.4)

Also, transmitted signal power $(=\sigma_d^2)$, comprises transmit and channel power $(=K)$, and channel frequency response of kth sub-carriers $(=H_k)$. This above Equation 3.1.1.4 is used to control VCO which in turn the frequency synchronization can be maintained.

- **CFO estimation techniques using Training Symbol**

We know within the range of $\{|\varepsilon| < 0.5\}$, the above technique is valid for the estimation of CFO. But at the initial stage of the synchronization, for the estimation of wider CFO range, we have to go for this technique. The distance between two blocks of samples for correlation can be reduced by increasing the range of CFO estimation. This is only possible if only the technique where training symbols that are repetitive with some shorter period are applied. Let *D* be an integer that indicate the ratio of OFDM symbol length to the length of repetitive pattern. Suppose transmitter transmitting the training symbols with *D* repetitive patterns in the time-domain which can be formed by taking the IFFT as:

$$X_l[k] = \begin{cases} A_m, \ if \ k = D.i, i = 0,1, \dots \dots, \left(\frac{N}{D-1}\right) \\ 0, \qquad otherwise \end{cases}$$

(3.1.1.5)

Here, $A_m = M$-ary symbol and $\frac{N}{D}$ is an integer. As $x_l[n]$ and $x_l[n+N/D]$ are identical then, $y_l^*[n]y_l\left[n+\frac{N}{D}\right] = |y_l[n]|^{2e^{j\varepsilon\pi}}$, a receiver can make CFO, estimation as follows [31, 9].

$$\hat{\varepsilon} = \frac{D}{2\pi}\arg\{\sum_{n=0}^{\frac{N}{D}-1} y_l^*[n]y_l[n+N/D]\}$$

(3.1.1.6)

In this case range covered for the CFO estimation is $\{|\varepsilon \leq D/2|\}$ which becomes wider as *D* increases. In other hand the performance of the MSE might degrade as the number of samples for the computational of correlation is reduced by *1/D*. Hence, we can say that we improve the range of CFO estimation but there causes an negative effect in MSE performance. Thus we concluded that as MSE performance becomes worse when estimation range increases, we average the estimates with the repetitive patterns with shorter period as:

$$\hat{\varepsilon} = \frac{D}{2\pi}\arg\sum_{m=0}^{D-2}\sum_{n=0}^{\frac{N}{D}-1} y_l^*\left[n+\frac{mN}{D}\right]y_l\left[n+\frac{(m+1)N}{D}\right]$$

(3.1.1.7)

3.2.2 Frequency-Domain Estimation

When two training symbols are transmitted consecutively, then;

$$y_2[n] = y_1[n]e^{\frac{j2\pi N_\varepsilon}{N}} \quad \leftrightarrow \quad Y_2[k] = Y_1[k]e^{j2\pi\varepsilon}$$

(3.2.2.1)

Using above relationship, we get the CFO estimation as:

$$\hat{\varepsilon} = \frac{1}{2\pi}\tan^{-1}\{\sum_{k=0}^{N-1}\mathrm{Im}[Y_1^*[k]Y_2[k]]/\sum_{k=0}^{N-1}\mathrm{Re}[\ Y_1^*[k]Y_2[k]]\}$$

(3.2.2.2)

This above equation is a well known approach from Paul H. Moose [30]. The range for the CFO estimation is $|\varepsilon| \leq \frac{\pi}{2\pi} = 1/2$, it can be increased *D* times by using training symbol with *D* repetitive patterns. In this case above Equation 3.2.2.2 is applied to sub-carriers with non-zero values and then averaged over the sub-carriers. In this case also, MSE performance may degrade due to reduced number of non-zero samples taken during averaging in the frequency domain and also preamble period is required for the estimation of CFO.

3.2 REVIEW OF THE ALGORITHMS PROPOSED

CFO can produce Inter Carrier Interference (ICI) which can be much worse than the effect of noise on OFDM systems. That is why various CFO estimation and compensation algorithms have been proposed. An overview of all the algorithms mentioned below has been described in details.

3.2.1 Schmidl and Cox Algorithm

The estimation scheme of Schmidl and Cox [31] is shown in Figure 3.2.1.1. Schmidl and Cox [31] propose the use of two OFDM symbols for frequency synchronization similar to Moose [30]. However, these two OFDM symbols have special constructions that allow the frequency offset estimation larger than several sub-carriers spacing. In time domain, the first OFDM symbol consists of two identical symbols generated in the frequency domain by a PN sequence on the even sub-carriers and zeros on the odd sub-carriers. The differentially modulated PN sequence on the odd sub-carriers and another PN sequence on the even sub-carrier are holded on the second training symbol.

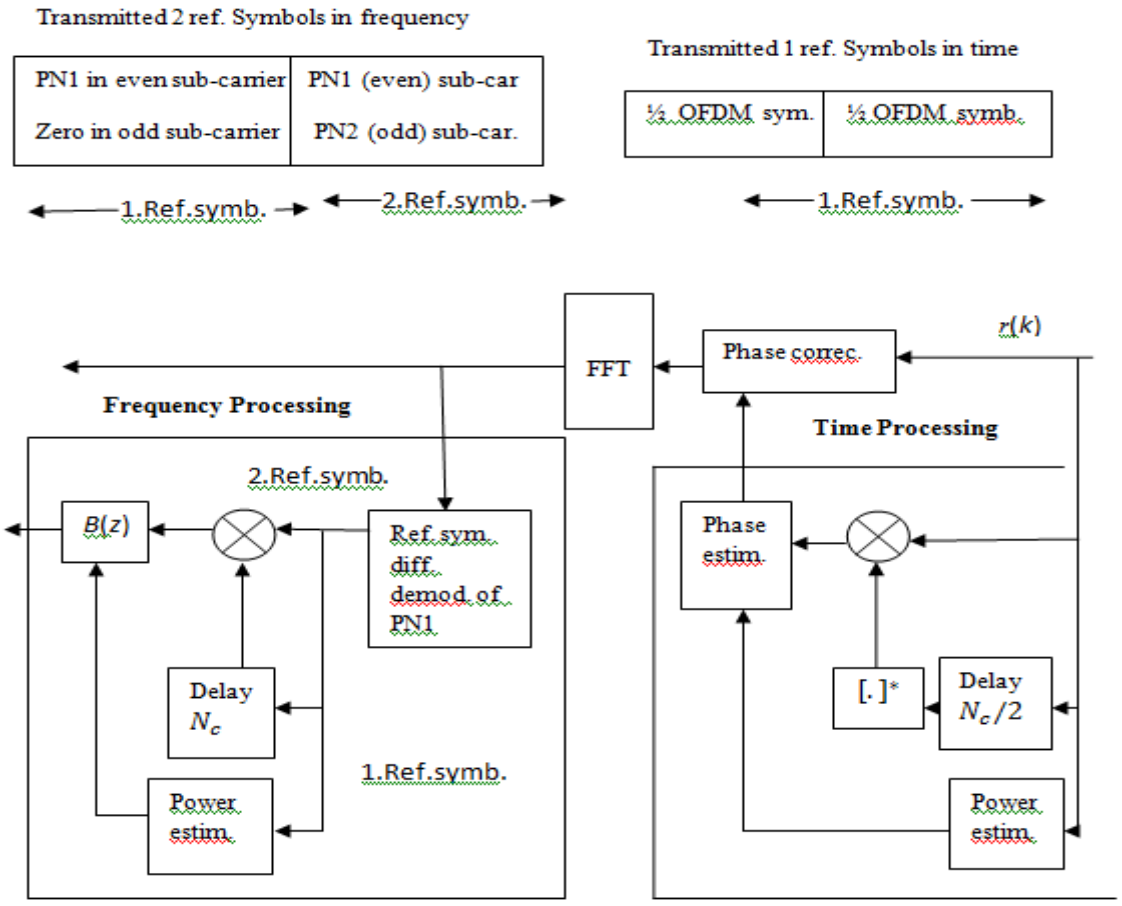

Figure 3.2.1.1 Schmidl & Cox Frequency Offset Estimation using 2 OFDM Symbols

Frequency offset Estimator:

Schmidl and Cox [31] designed two training symbols as preamble. The first one has two identical parts $S_{1,n}$ and $S_{1,n+L}$ with $\frac{N}{2}$ samples each and $L = \frac{N}{2}$ delay between identical samples. They will remain identical after passing through the channel, except the phase difference Δf between them due to the frequency offset (Δf_c). The received two parts of training symbol are:

$$r_{1,n} = S_{1,n}.e^{j2\pi\Delta f_c nT_s} + \eta(nT_s) \qquad \textbf{(3.2.1.1)}$$

$$r_{1,n+L} = S_{1,n+L}.e^{j2\pi\Delta f_c (n+L)T_s} + \eta(nT_s)$$

$$= r_{1,n}.e^{j2\pi\Delta f_c LT_s} + \eta(nT_s) \qquad \textbf{(3.2.1.2)}$$

Consequently, without noise, the two parts will have the following relation:

$$r_{1,n+L} = r_{1,n}.e^{j2\pi\Delta f_c LT_s}$$

(3.2.1.3)

Now the phase of their correlation is also given as:

$$\emptyset = 2\pi.\Delta f_c LT_s = \pi.\Delta f_c NT_s$$

(3.2.1.4)

Now, $\emptyset$ can be estimated at the best timing point as:

$$\emptyset = angle\big(P(d)\big)$$

(3.2.1.5)

Also, if $|\emptyset|$ is less than π, then the frequency offset estimate is given by,

$$f_e = \frac{\emptyset}{\pi NT_s}$$

(3.2.1.6)

Otherwise, the actual frequency offset is estimated by;

$$f_e = \frac{\emptyset}{\pi NT_s} + \frac{2l'}{NT_s}$$

(3.2.1.7)

where, l' is an integer. To find the unknown second term in Equation 3.2.1.7, the training symbol are partially corrected with the known frequency offset by multiplying the samples with

$$e^{-\frac{j2\pi\emptyset t}{\pi NT_s}} = e^{-\frac{j2\emptyset t}{NT_s}}$$

(3.2.1.8)

Let the FFT's of the received first and second offset frequency corrected training symbols $(F_{1,k}, F_{2,k})$ and the differentially modulated even frequencies of the second training symbol be (u_k). The sliding correlation between the FFT's and (u_k) is given by

$$B(l) = \frac{\left|\sum_{k\in X} F^*_{1,k+2l} u^*_k F_{2,k+2l}\right|^2}{2\left(\sum_{k\in X}\left|F_{2,k}\right|^2\right)^2}$$

(3.2.1.9)

where, X is the set of indices for even frequency components of the second training symbol. Finally, the l corresponding to the maximum value of $B(l)$ is used to calculate integral frequency offset in Equation 3.2.1.7.

3.2.2 Best Linear Unbiased Estimator (BLUE)

Michele Morelli *et al*. [32] extended the Schmidl and Cox algorithm for the estimation of CFO where it need one training symbol. The proposed estimator exploits the correlations of the samples from the matched filter. The estimated frequency offset ($\hat{v}$) is expressed as:

$$\hat{v} = \frac{1}{\frac{2\pi}{L}} \sum_{m=1}^{H} w(m)\varphi(m)$$

(3.2.2.1)

where, H is a design parameter less than or equal to $L-1$, and $w(m)$ is the m^{th} component of;

$$w = \frac{C_\varphi^{-1} 1}{1^T C_\varphi^{-1} 1}$$

(3.2.2.2)

In this equation, C_φ is the covariance matrix of $\varphi \triangleq [\varphi(1), \varphi(2), \ldots\ldots\ldots\ldots, \varphi(H)]^T$ and $1 \triangleq [1,1, \ldots\ldots, 1]^T$ is the H-dimensional column vector of all ones. The variance of BLUE is,

$$var\{\hat{v}\} = \frac{1}{\left(\frac{2\pi}{L}\right)^2} \frac{1}{1^T C_\varphi^{-1} 1}$$

(3.2.2.3)

To explain the basic idea, let us consider angle as:

$$\varphi(m) \triangleq [\arg(R(m)\} - \arg\{R(m-1)\}]_{2\pi,} \qquad for\ 1 \le m \le H$$

(3.2.2.4)

where $[x]_{2\pi}$ denote modulo-2π operation (it reduces x to the interval $[-\pi, \pi)$, arg $\{R(m)\}$ is the argument of $R(m)$. The $R(m)$ as:

$$R(m) = \frac{1}{N - mM} \sum_{k=mM}^{N-1} x(k)x^*(k - mM), \qquad 0 \le m \le H$$

(3.2.2.5)

Here, $M = N/L$ is the length (in sampling intervals) of each section of the training symbol.

3.2.3 Chirp Training Symbol Based Estimator

In this scheme, the CAZAC (Constant Amplitude Zero Auto-Correlation) uses chirp signal or training symbol [33].

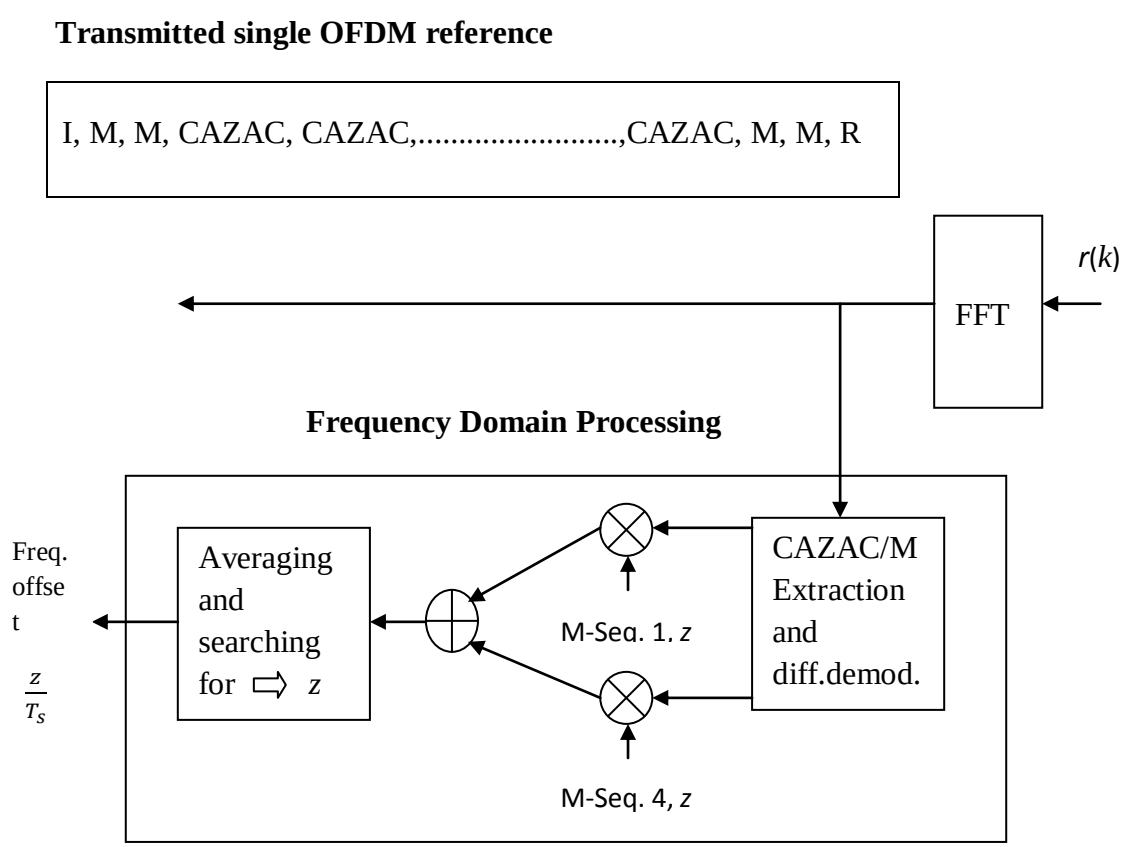

Figure 3.2.3.1 Coarse Frequency Offset Estimation based on CAZAC/M Sequences.

As shown in Figure 3.3.1, CAZAC/M sequences are generated in frequency domain and are embedded in I and R sequences. The CAZAC/M sequences are differentially modulated. The length of CAZAC sequences is much smaller than the length of M sequences. The I and R sequences have same length N_1, and used as the start position for the differential encoding/decoding of M sequences. It uses only one OFDM reference symbol but high amount of computation is needed. The coarse synchronization is achieved by correlating with the transmitted known M sequence reference data shifted over $\pm N_1$ sub-carriers and then result from different sequences are averaged.

L.Wei *et al.* [33] proposed two CAZAC sequences or chirp signal for the preamble purpose. The first sequence is used for FFO estimation. The first and second sequences are both utilized for IFO estimation after compensation. The CAZAC sequence in time-domain as:

$$x(n) = exp\left(\frac{j\pi r n^2}{N}\right), \qquad for\ n = 0,1, \dots \dots, N-1$$

(3.2.3.1)

where, parameter of CAZAC sequence $(= r)$. The FFO is estimated using the autocorrelation of the received signal. The IFO estimation is based on the fact that DFT of a CAZAC sequence is also known as CAZAC sequence. Defining
$X(k) = \{X(0) \dots \dots \dots \dots X(N-1)\} = FFT\big(x(n)\big),\ \ x(n) = \{x(0) \dots \dots \dots \dots x(N-1),$ we have:

$$Z_k = \frac{1}{\sqrt{N}} \sum_{n=0}^{N-1} \left(y(n) e^{-\frac{j2\pi \hat{\varepsilon}_f n}{N}} \right) e^{-\frac{j2\pi kn}{N}}$$

(3.2.3.2)

$$R_f\big(\varepsilon - \hat{\varepsilon}_f, r, \tau\big) = \frac{1}{N} \sum_{k=0}^{N-1} X(k-\tau)_{mod} Z^*(k)$$

(3.2.3.3)

Now, after the normalized integer fractional frequency offset $\hat{\varepsilon}_i$ will be estimated using following steps:

Step 1: Find the peak location of the two correlations respectively.

$$L_{1\,max} = argmax_{\tau}\{|R_f(\varepsilon - \hat{\varepsilon}_f, r_1, \tau)|\}$$

(3.2.3.4)

$$L_{2\,max} = argmax_{\tau}\{|R_f(\varepsilon - \hat{\varepsilon}_f, r_2, \tau)|\}$$

(3.2.3.5)

Step 2: $If\ L_{1\ max} < \frac{N}{2}$, go to step 3, else go to step 4.

Step 3: $While\left(L_{2\,max} \geq \frac{N}{2}\right)$

$$\{L_{2\,max} = (L_{2\,max} + r_2)_{mod\ N}\}$$

(3.3.3.6)

$While\ (L_{2max} < L_{1max})$

$$\{L_{2\,max} = (L_{2\,max} + r_2)\}$$

(3.2.3.7)

Go to step 5.

Step 4: $While\ (L_{2\,max} < L_{1\,max})\ and (L_{2\,max} > r_2)$

$$\{L_{2\,max} = (L_{2\,max} + r_2)\}$$

(3.2.3.8)

Step 5: $\hat{\varepsilon}_i = (L_{2\,max})_{mod\ N}$

$$if\ \hat{\varepsilon}_i > \frac{N}{2}, \hat{\varepsilon}_i = \hat{\varepsilon}_i - N \quad \left(assuming\ |\varepsilon| < \frac{N}{2}\right)$$

(3.2.3.9)

3.2.4 Joint Maximum Likelihood (ML) Symbol time and Carrier frequency offset Estimator

Jan-Jaap Van de Beek *et al.* [34] proposed a CFO estimation making use of the time-domain cyclic prefix. Here, in the case of blind CFO estimation algorithm, the CFO is estimated by using the statistical properties of the received signal only, without detail information of transmitted signal. Also, blind CFO estimation algorithms make use of

some special properties of the OFDM symbols such as guard null sub-carriers in the frequency domain and cyclic prefix in the time domain.

Notice that all sub-carriers experiences the same shift ε, these two uncertainties and the AWGN thus yield the received signal:

$$r(k) = s(k-\theta)e^{\frac{j2\pi\varepsilon k}{N}} + n(k)$$

(3.2.4.1)

Also the samples in the cyclic prefix and their copies $r(k)$ are pair wise correlated, and based on above equation, it has following property.

$$E\{r(k)r^*(k+m)\} = \sigma_s^2 \exp(j2\pi\varepsilon) + \sigma_n^2$$

(3.2.4.2)

Based on this property, the maximum likelihood (ML) CFO estimator is given by;

$$\hat{\varepsilon} = \frac{1}{2\pi} < \left(\sum_{k=m}^{m+L-1} r(k)r^*(k+m) \right)$$

(3.2.4.3)

where, m is the start of the cyclic prefix of the received signal. From above Equation (3.2.4.3), we see that CFO estimation requires the computational of the autocorrelation of the received signal, as computational complexity is low. The acquisition range in this method is limited to ± 0.5 sub-carrier spacing and MSE of the CFO estimation also degrades.

3.2.5 Data Driven Technique

Paul H. Moose [30] has shown the effect of offset errors on signal to noise and then presented an algorithm to estimate the offset. In this algorithm, two repetitive OFDM symbols are sent which works on the knowledge of the starting point of OFDM symbol. Now, the maximum likelihood estimate (MLE) of CFO given as:

$$\hat{\varepsilon} = \frac{1}{2\pi} \tan^{-1} \left\{ \frac{(\sum_{k=-K}^{K} Im[Y_{2k} Y_{1k}^*])}{(\sum_{k=-K}^{K} Re[Y_{2k} Y_{1k}^*])} \right\}$$

(3.2.5.1)

where, the MLE for CFO $(= \hat{\varepsilon})$, $\boldsymbol{Im}$ is the imaginary part, $\boldsymbol{Re}$ is the real part, and $*$ is complex conjugate. In this estimation, the mean square error as:

$$Mean\ square\ of\ [\hat{\varepsilon}] = \frac{1}{(2\pi)^2 N\mu}$$

(3.2.5.2)

where, the total number of sub-carriers $(= N)$, and the ratio of the signal to noise for the received signal(=μ).Also acquisition range is$|\varepsilon| \leq 0.5 = (-0.5 \leq Acquisition\ range \leq 0.5)$ which is smaller than the value that is in IEEE 802.11a. Due to the discontinuity of the arctangent and noise, the acquisition range going toward 0.5 may jumps to -0.5. When this happens, practically it becomes useless and the estimate is no longer unbiased.

3.2.6 Blind CFO Estimation Technique using ESPRIT Algorithm

Ufuk Tureli *et al.* [35] proposed the shift invariant structure to estimate the parameters for generating the eigenvalues calculation. The m^{th} block of the received signal minus prefix as:

$$y(m) \stackrel{\text{def}}{=} [y_0(m) \dots \dots \dots . . y_{N-1}(m)]^T$$

(3.2.6.1)

Here, from above equation, the samples in forward and backward direction can be considered respectively:

$$y_F^i(m) \stackrel{\text{def}}{=} [y_{i-1}(m)\ \ y_i(m) \dots \dots \dots \dots y_{i+L-1}(m)]^T$$

(3.2.6.2)

$$y_B^i(m) \stackrel{\text{def}}{=} [y_{N-i}(m)\ \ y_{Ni}(m) \dots \dots \dots \dots y_{N-i-L}(m)]^H$$

(3.2.6.3)

where, $i = 1,2, \dots \dots, N - L$and $[.]^H$ means conjugate is transpose. Now N point received signal is expressed as:

$$y(m) = EW_pH_pS(m)e^{j(m-1)\varphi(N+N_g)}$$

(3.2.6.4)

Now from definition, $\check{S}(m) = H_pS(m)e^{j(m-1)\varphi(N+N_g)}$, therefore $y(m) = W_pE\check{S}(m)$ and

$$E = diag\left(1, e^{j\varphi}, \dots\dots\dots\dots\dots\dots, e^{j(N-1)\varphi}\right)$$

(3.2.6.5)

It can be shown that:

$$y_F^i(m) = E_{L+1} W_{L+1} \Delta^i \check{S}(m)$$

(3.2.6.6)

where, $E_{L+1} = diag\left(1, e^{j\varphi}, \dots\dots\dots\dots\dots\dots, e^{jL\varphi}\right)$ and the diagonal matrix can be written as $\Delta = diag\left(1 + e^{j(w+\varphi)}, \dots\dots\dots\dots\dots, e^{j(P-1)w+\varphi}\right), where, w = \frac{2\pi}{N}$.

In the same way, backward vector can be as:

$$y_B^i(m) = E_{L+1} W_{L+1} \Delta^i \times e^{-j\varphi(N-1)} \begin{bmatrix} 1 & \cdots & 0 \\ \vdots & \ddots & \vdots \\ 0 & \cdots & e^{j(P-1)(N-1)w} \end{bmatrix}$$

(3.2.6.7)

Here, $r(m) \stackrel{\text{def}}{=} e^{-j\varphi(N-1)} \begin{bmatrix} 1 & \cdots & 0 \\ \vdots & \ddots & \vdots \\ 0 & \cdots & e^{j(P-1)(N-1)w} \end{bmatrix}$ therefore;

$$y_B^i(m) = E_{L+1} W_{L+1} \Delta^i r(m)$$

(3.2.6.8)

The operator $[.]^*$ mean complex conjugate. By considering $A_{L+1} \stackrel{\text{def}}{=} E_{L+1} W_{L+1}$, the covariance matrix as:

$$R_{L+1} \stackrel{\text{def}}{=} \frac{1}{K(N-L)} = \sum_{m=1}^{M} \sum_{i=1}^{N-L} \left[y_F^i(m) \left(y_F^i(m)\right)^H + y_B^i(m) \left(y_B^i(m)\right)^H \right]$$

$$= A_{L+1} \varepsilon \left[\left(\check{S}(m) + r(m)\right) \left(\check{S}(m) + r(m)\right)^H \right] A_{L+1}^H$$

(3.2.6.9)

The p eigenvectors of A_{L+1} can be found by using the Spectral Value Decomposition (SVD). However, the carrier frequency offset in this case can be as:

$$\exp(j\varphi) = \frac{tr(\Delta)}{\sum_{m=0}^{P-1} \exp(jmw)}$$

(3.2.6.10)

where, $w = 2\pi/N$, and CFO can be computed as:

$$\varphi = Angle\left(\frac{Trace(\Delta)}{\sum_{m=0}^{P-1}\exp(jmw)}\right)$$

(3.2.6.11)

3.2.7 CFO Estimation Using Periodic Preambles

Yu and *et. al.* [36] proposed an algorithm which contains step such as: constructing the correlation matrix, calculating coefficient for correlation matrix, finding non-zero roots, and finally finding CFO. Now the received preamble to the receiver is expressed as:

$$y(m) = e^{\frac{j2\pi\varepsilon mx(M)}{N}} + w(m)$$

(3.2.7.1)

where, $w(m)$ is additive white Gaussian noise (AWGN), ε is CFO, and $x(M) = s(m) * h(m)$. Since $s(m)$ is preamble signal with period N and length QN, where $m = 0,1,2,\ldots\ldots, QN-1$, $h(m)$ is channel response, and $x(M)$ is output signal from transmitter. However, $y(n), X(n), and\ W(n)$ can be given as:

$$y(n) = [y_1(n)\ \ y_2(n)\ \ \ldots\ldots\ldots y_m(n)]^T$$

$$X(n) = [x_1(n)\ \ x_2(n)\ \ \ldots\ldots\ldots x_m(n)]^T$$

$$W(n) = [w_1(n)\ \ w_2(n)\ \ \ldots\ldots\ldots w_m(n)]^T$$

(3.2.7.2)

And

$$Y = [y(0)\ \ y(1)\ldots\ldots.\ y(N-1)]$$

$$X = \left[X(0)\ \ X(1)e^{\frac{j2\pi\varepsilon}{N}}\ \ldots..\ X(N-1)e^{\frac{j2\pi\varepsilon(N-1)}{N}}\right]$$

$$W = [W(0)\ \ W(1)\ldots\ldots.\ W(N-1)]$$

$$A = \begin{bmatrix} e^{j2\pi\varepsilon} & \cdots & 0 \\ \vdots & \ddots & \vdots \\ 0 & \cdots & j2\pi\varepsilon M \end{bmatrix}$$

(3.2.7.3)

Now, Equation 3.2.7.1 can be stated as:

$$Y = AX + W$$

(3.2.7.4)

According to algorithm, X should be estimated by LS method and then CFO by using ML function. Now, LS estimate of X as:

$$X_{LS} = \left(\frac{1}{M}\right) A^H Y = A + Y$$

(3.2.7.5)

where, A^H is Hermitian operation and substituting the value of X_{LS} in Equation 3.2.7.4, we get,

$$\sum_{n=0}^{N-1} \|y(n) - AA + y(n)\|^2 = N.trace\left((I - AA^+)R_y\right)$$

(3.2.7.6)

where, I is the identity matrix, and $R_y = E[YY]^H$. The CFO estimation based on this algorithm can be obtained as:

$$\hat{\varepsilon} = \frac{1}{j2\pi} \ln(\hat{z})$$

(3.2.7.7)

Here, $\hat{z} = \arg\{\max_{z \in \circ}(A(z))\}$ and $|\hat{z}| = 1$, since it has high computational complexity due to the root finding procedure.

3.2.8 CFO Estimation Techniques Using Classen Method

Classen et al. **[37]** proposed the CFO tracking where every OFDM symbol are transmitted as well as pilot tones are inserted in the frequency domain. In the below Figure 3.2.8.1, shows the structure of CFO using pilot tones. Firstly, two OFDM symbols, $y_l[n]$ and $y_l[n + D]$ are saved in the memory after synchronization. Then, the signals are converted into $\{Y_l[k]\}_{K=0}^{N-1}$ and $\{Y_{l+D}[k]\}_{K=0}^{N-1}$ via FFT, from which pilot tones are extracted. After estimating CFO from pilot tones in the frequency domain, the signal is compensated with the estimated CFO in the time domain. In this process, two different estimation modes for CFO estimation is implemented: acquisition and tracking modes. In the acquisition mode, a large range of CFO including and integer CFO is estimated. In the tracking mode, only fine CFO is estimated. The integer CFO is estimated as:

$$\hat{\varepsilon}_{acq} = \frac{1}{2\pi . T_{sub}} max \left\{ \left| \sum_{j=0}^{L-1} Y_{l+D}[p[j], \varepsilon] Y_l^*[p[j], \varepsilon] X_{l+D}^*[p[j] X_l[p[j]] \right| \right\}$$

(3.2.8.1)

where, $L, p[j], and\ X_l[p[j]]$ denote the number of pilot tones, the location of the j^{th} pilot tone, and the pilot tone located at

$$\hat{\varepsilon}_f = \frac{1}{2\pi . T_{sub} . D} arg \left\{ \left| \sum_{j=1}^{L-1} Y_{l+D}[p[j], \hat{\varepsilon}_{acq}] Y_l^*[p[j], \hat{\varepsilon}_{acq}] X_{l+D}^*[p[j] X_l[p[j]] \right| \right\}$$

(3.2.8.2)

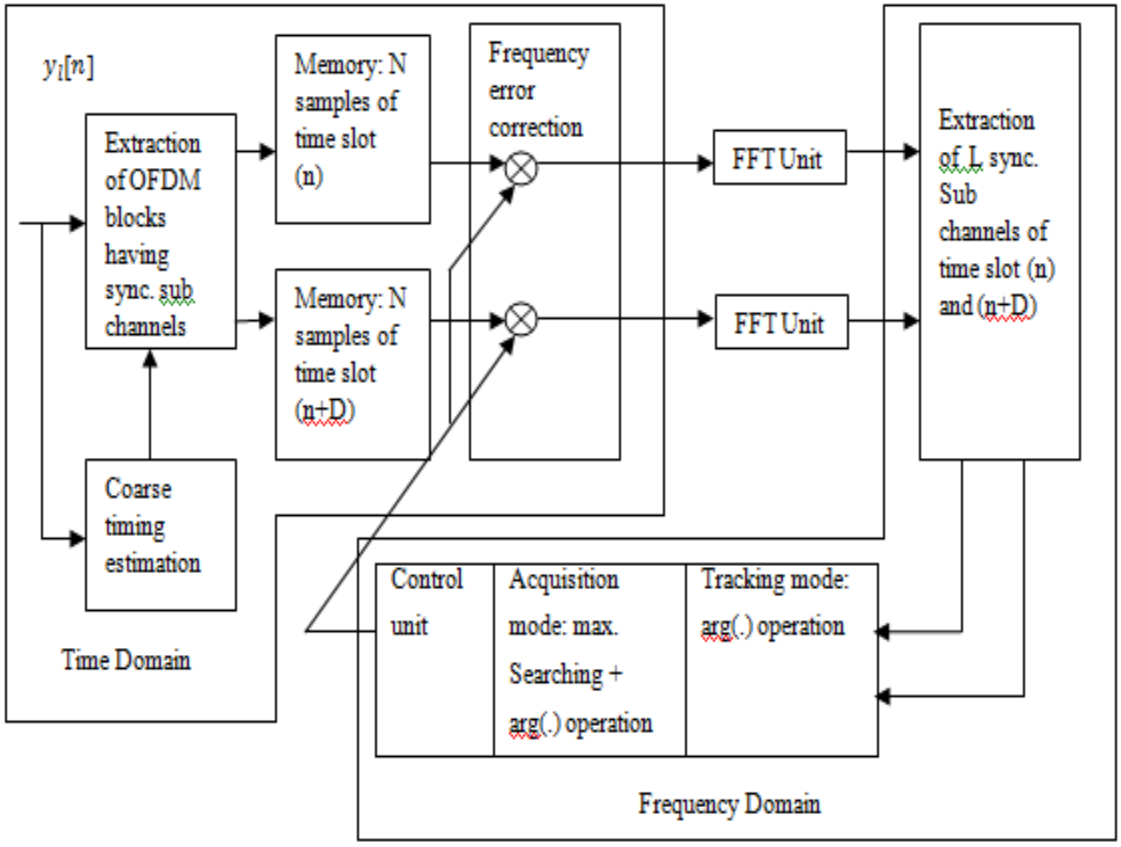

Figure 3.2.8.1 CFO Synchronization Scheme Using Pilot Tones.

In the acquisition mode, $\hat{\varepsilon}_{acq}$ and $\hat{\varepsilon}_f$ are estimated and then, the CFO is compensated by their sum. In the tracking mode, only $\hat{\varepsilon}_f$ is estimated and then compensated.

CHAPTER 4 RESULTS AND ANALYSIS

In this chapter, the performance of the OFDM systems in the presence of frequency offset between the transmitter and the receiver has been analysed in terms of mean squared error (MSE) and the signal to noise ratio (SNR) performance. Inter carrier interference (ICI) which results from the frequency offset between the frequencies of transmitter and the receiver oscillators degrades the performance of the OFDM system. Three different methods CFO-CP, Moose, and Classen were analyed in this chapter on the basis of different frequency offset values.

4.1 RESULTS

Performances of estimation techniques vary depending on the number of samples in CP, the number of samples in preamble/Moose, and the number of pilot tones/Classen used for CFO estimation. The simulations are performed to verify the accuracy of MSE analysis. Now the simulation result has been performed by considering system parameters as shown in Table 4.1.1.

Table 4.1.1 Parameters and its Specifications

Parameter	Specifications
FFT size	128
Modulation Scheme	QPSK
Channel	AWGN
Guard Length/CP	32
Number of bits per symbol	2
Frequency offset	0.10, 0.15,0.30
Number of Carriers in OFDM symbol	128+32=160
Symbol Duration	3

In simulated Figure 4.1.1, shows MSE performance for three different techniques with taking CFO=0.10, 0.15, and 0.30. According to MATLAB Figure 4.1.1; Classen method is better than CP and Moose method.

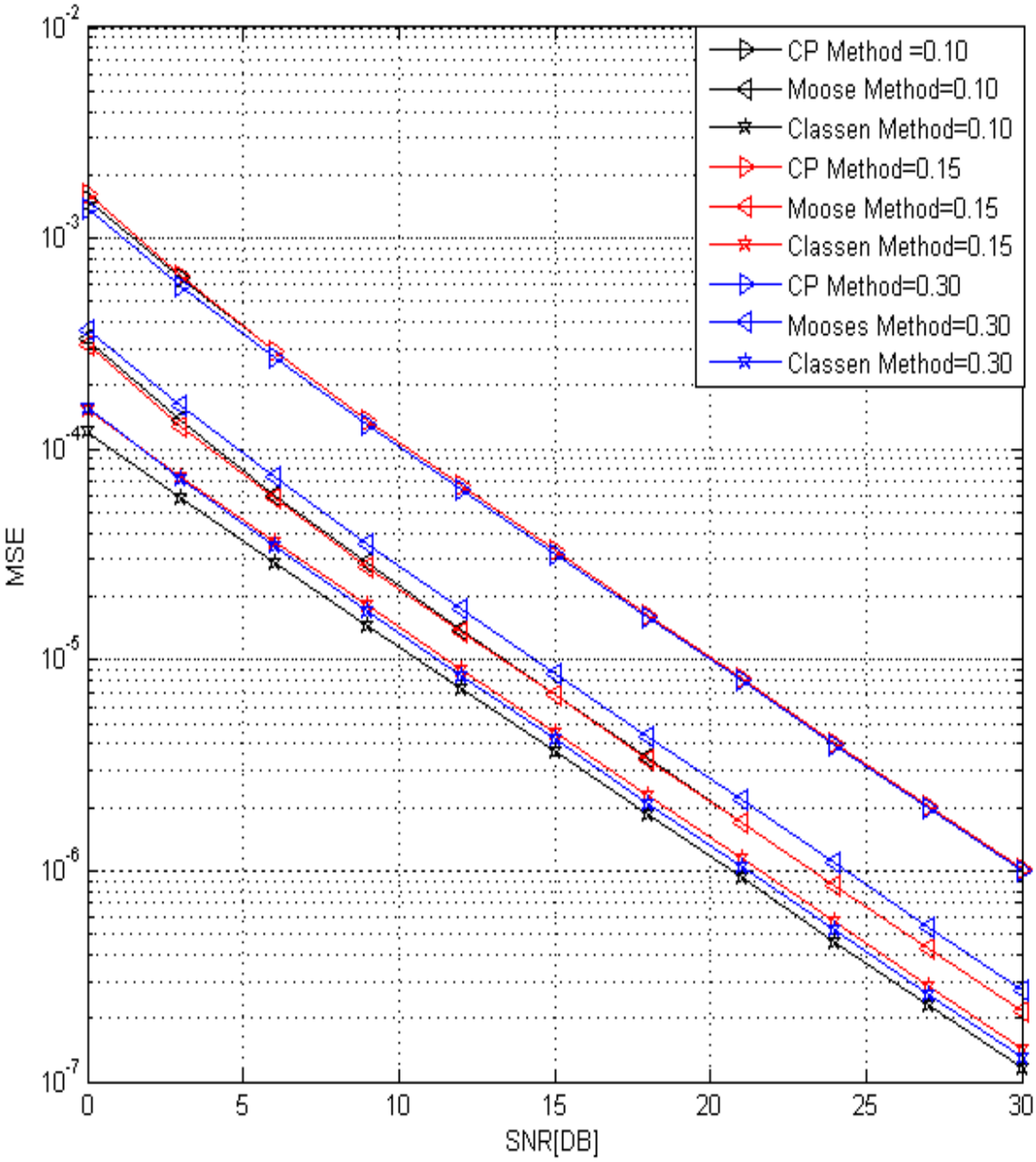

Figure 4.1.1 MSE of CFO Estimation Techniques

Now, from simulated results, the result of MSE at 30 dB SNR is compared among the three different methods as:

Table 4.1.2 Performance Comparison of different Methods at 30 dB SNR

Frequency Offset	Methods Used	MSE
0.1	CP	1.001×10^{-6}
	Preamble	2.146×10^{-7}
	Pilot	1.66×10^{-7}
0.15	CP	1.001×10^{-6}
	Preamble	2.146×10^{-7}
	Pilot	1.434×10^{-7}
0.30	CP	1.001×10^{-6}
	Preamble	2.718×10^{-7}
	Pilot	1.31×10^{-7}

4.2 ANALYSIS

The first technique we use for synchronization is done by exploiting the OFDM symbol; in particular CP. But there is a problem that it can only estimate a limited CFO within the range of $|\alpha| \leq 0.5$. Therefore, the training symbols are used and corresponding phase difference in actual symbol and training symbol is measured and hence CFO. Now Moose model has much more range given by $|\alpha| \leq 0.5$, but it can also be increased D times, where D is the number of repetitive patterns. Now, in Classen method, MSE is further decreased but there is trade off as with the increase in performance complexity also increases. With CP, we have least complexity as number overhead is required, then the complexity is increased in Moose and Classen methods.

4.3 CONCLUSION

We investigated the performance of three frequency offset estimators for wireless OFDM systems. From above results, the pilot based estimator has best performance in MSE at different frequency offset. CP based estimator has worst performance because of easy implementation and no loss of bandwidth efficiency, and also MSE is same at different frequency offset. Although preamble based estimator has nearby similar performance as pilot based estimator in terms of MSE.

CHAPTER 5 CONCLUSION & FUTURE SCOPE

The objective of this thesis was to perform a detailed study of the problem of frequency synchronization that forms the major difficulty in the practical implementation of the OFDM system.

5.1 CONCLUSION

A broad background of OFDM based communication systems was presented in the chapter 1, including the sub-carrier orthogonality requirement, IFFT/FFT processes, and historical background of the system. OFDM works on the principle of orthogonality, sub-carriers are orthogonal to each other. This orthogonality between sub-carriers may be destroyed if carrier frequency offset arises between them due to Doppler spreading while transmission. Due to its advantages features like immunity to delay spread, simple equalization, efficient bandwidth usage, and resistance to frequency selective fading; the OFDM has been adopted by many wireless communication standards like IEEE 802.16, IEEE 802.11a, DAB, DVB-T, WLL communication system. Besides these, there are some disadvantages of OFDM which must be resolved. Therefore, for overall improvement in the performance of OFDM system, it is required to handle all these issues properly. The main focus of work was to provide an appropriate solution to each and every major problems related to frequency synchronization. In chapter 2, a theoretical analysis of frequency synchronization and their effects on overall system performance were examined. The main task of frequency synchronization in OFDM system is to estimate and correct this carrier frequency offset at the receiver, and also reveals the details on OFDM system model along with its parameters. Chapter 3, includes the mathematical analysis of the CFO techniques used, and some of the algorithms that have been proposed in the past including their qualitative and quantitative analysis.

Chapter 4 covers the MATLAB simulation of the three different algorithms and its comparisons with time domain CP method and frequency domain (Moose/Classen) method terms of MSE vs SNR. Performance of estimation techniques vary depending on the number of samples in CP, the number of samples in preamble, and the number of pilot tones, used in CFO estimation.

5.2 FUTURE SCOPE

The work that has been done in this thesis involves the algorithms that basically deal with the rectification of the problem of frequency synchronization which is the major obstruction in the pathway of practical implementation of OFDM systems. We also concluded that phase lock loop (PLL) should be included in the estimator to increase the accuracy and stability of estimated frequency and phase offset. Further demanding research is needed in MIMO-OFDM system allowing for the generalized system model, where the CFO and propagation delay between each transmit antenna and receive antenna are possibly different.

Recently, a new OFDM system based on a combination of CDMA and OFDM signalling, referred to as MC-CDMA system, has gained much attention. A MC-CDMA system can provide higher capacity for multiple accesses and still hold the advantage of OFDM such as robustness for frequency selective fading. Hence, the synchronization scheme under MC-CDMA system is also worth of future study. Besides it, we have planned to merge this scheme with the combining scheme such as Maximum Ratio Combining, Equal Ratio Combining, and Selective Ratio Combining and so on. Among these the perfect dimension which will match with our scheme will be on work on future.

REFERENCES

[1] Richard Van Nee and Ramjee Prasad, "OFDM for Wireless Multimedia Communications," Artec House Publishers, London, 2000.

[2] Arvind Kumar and Rajoo Pandey, "A Bandwidth Efficient Method for Cancellation of ICI in OFDM Systems," *International Journal of Electronics Communication*, vol. 63, pp. 569-575, 2009.

[3] IEEE Std.802.11a, "Wireless Medium Access Control (MAC) and Physical Layer (PHY) specifications: High Speed Physical Layer Extension in the 5 GHZ Band," *IEEE*, 1999.

[4] R. R. Moiser and R. G. Clabaugh, "Kineplex a Bandwidth Efficiency Binary Transmission System," *AIEE Transactions*, vol. 76, pp. 723-728, 1958.

[5] R. Prasad and L. Gavrilovska, "Research Challenges for Wireless Personal Area Networks," *Proceedings* of *3rd International Conference on Information, Communications and Signal Processing (ICICS)*, Singapore, 2001.

[6] "Orthogonal Frequency Division Multiplexing," United States Patent No. 3, 488, 4555, filed November 14, 1966, issued January 6, 1970.

[7] M. Speth, "OFDM Receivers for Broadband-Transmission," Internet article: http: //www.ert.rwth − aachen.de/Projekte/Theo/OFDM/www ofdm.html, 2001.

[8] T. Pollet, M. van Bladel and M. Moeneclaey, "BER Sensitivity of OFDM Systems to Carrier Frequency Offset and Wiener Phase Noise", *IEEE Transactions on Communication*, pp.191-193, 1995.

[9] K. Taura, M. Tsujishta and M. Takeda, "A digital Audio Broadcasting (DAB) Receiver," *IEEE Transactions on Consumer Electronics*, vol. 42, no. 3, pp. 322-326, 1996.

[10] F. Daffara and O. Adami, "A New Frequency Detector for Orthogonal Multi-Carrier Transmission Techniques," *in Proceedings of Vehicular Technology Conference, Chicago, IL*, vol. 2, pp. 804-809, 1995.

[11] Haitham J. Taha and M. F. M. Salleh, "ICI Self-Cancellation for FFT-OFDM System," *Australian Journal of Basic and Applied Sciences*, vol. 4, no.11, pp. 5621-5629, 2010.

[12] D. Parsons, "The Mobile Radio Propagation Channel," New York: John Wiley & Sons, Inc., 1992.

[13] S.D. Sandberg, "Overlapped Discrete Multi-Tone Modulation for High Speed Copper Wire Communications," *IEEE Journal of Selected Areas Communication*, vol.13, no.9, pp. 1571-1585, 1995.

[14] K. Fazel and K. Kaiser, "Multi-Carrier and Spread Spectrum Systems," 2008.

[15] J. G. Proakis, "Digital Communications," New York: McGraw-Hill, 1995.

[16] S. D. Sandberg, "Overlapped Discrete Multi-Tone Modulation for High Speed Copper Wire Communications," *IEEE Journal Selected Areas Communication*, vol. 13, no. 9, pp.1571-1585, 1995.

[17] R.W. Chang, "Synthesis of Band-Limited Orthogonal Signal for Multichannel Data Transmission," *Bell System Technical Journal*, pp.1775-1796, 1996.

[18] Web ProForum, "OFDM for Mobile Data Communications," Online Tutorial, Internet address: http://www.ice.org/2000.

[19] IEEE P802.16, Part 16: "Air Interface for Fixed Broadband Wireless Access Systems," *Revision of IEEE Std. 802.16-2004 as amended by IEEE Std. 802.16f-2005 and IEEE Std. 802.16e-2005*, Mar. 2007.

[20] Taewon Hwang, Chenyang Yang, Gang Wu, Shaoqian Li, and Geoffrey Ye Li, "OFDM and its wireless Applications:A Survey," *IEEE Transactions on Vehicular Technoloagy*, vol. 58, no. 4, May 2009.

[21] H. D. Joshi and R. Saxena, "OFDM and its Major Concerns: A Study with Way OUT," *IETE Journal of Education*, vol. 54, no. 1, pp. 1-49, 2013.

[22] A. Peled and A. Ruiz, "Frequency Domain Data Transmission using Reduced Computational Complexity Modems," *Proceedings of IEEE International Conference on Accoustics, Speech, and Signal Processing (ICASSP)*, vol. 5, pp. 964–967, 1980.

[23] M. Bossert, A. Donder and V. Zyablov, "Improved Channel Estimation With Decision Feedback for OFDM Systems," *IEE Electronics Letters*, vol. 34, no. 11, pp. 1064–65, 1998.

[24] M. K. Ozdemir and H. Arslan, "Channel Estimation for Wireless OFDM Systems," *IEEE Communication Surveys Tutorials*, vol. 9, no. 2, pp. 18-48, 2007.

[25] S. Coleri, M. Ergen, A. Puri and A. Bahai, "Channel estimation techniques based on pilot arrangement in OFDM systems," *IEEE Transactions on Broadcasting*, vol. 48, pp. 223-229, 2002.

[26] B. Sklar, "Digital Communications: Fundamentals and Applications 2/E", Prentice Hall, 2002.

[27] P. Robertson, "Effects of Synchronization Errors on Multi-Carrier Digital Transmission Systems," *DLR Internal Report*, 1994.

[28] 3GPP TSG-RAN-1 Meeting #31, "Technical Description of the OFDM/IOTA Modulation," 2003.

[29] T. Pollet and M. Moeneclaey, "Synchronizability of OFDM Signals," *IEEE Globecom'95*, pp. 2054–2058, 1995.

[30] P.H. Moose, “A Technique for Orthogonal Frequency Division Multiplexing Frequency Offset Correction,” *IEEE Transactions on Communications*, vol.42, pp. 2908-2914, 1994.

[31] T. M. Schmidl and D. C. Cox, “Robust Frequency and Timing Synchronization for OFDM,” *IEEE Transactions on Communications*, vol. 45, pp. 1613-1621, 1997.

[32] M. Morelli and U. Mengali, “An Improved Frequency Offset Estimator for OFDM Applications,” *IEEE Communication Letters*, vol. 3, no. 3, pp. 75–77, 1999.

[33] L. Wei, Y.Y. Xu, Y.M. Cai and X. Xu , “Robust Frequency Offset Estimator for OFDM Over Fast Varying Multipath Channel,” *IEE Electronics Letters*, vol. 43, no. 6, pp. 53-54, 2007.

[34] J. van de Beek, M. Sandell and P. O. Baorjesson, “ML Estimation of Time and Frequency Offset in OFDM Systems," *IEEE Transactions on Signal Processing*, vol. 45, no. 7, pp. 1800-1805, 1997.

[35] Ufuk Tureli, Hui Liu and Michael D. Zoltowski, “OFDM Blind Carrier Offset Estimation: ESPRIT,” *IEEE Transactions on communications*, vol. 48, 2000.

[36] J. H. Yu and Y. T. Su, “Pilot-Assisted Maximum-Likelihood Frequency Offset Estimation for OFDM Systems,” *IEEE Transaction Communication*, vol. 52, no. 11, pp. 1997–2007, 2004.

[37] F. Classen, and H. Myer, “Frequency Synchronization Algorithm for OFDM Systems Suitable for Communication over Frequency Selective Fading Channels,” *IEEE VTC’94*, pp. 1655–1659, 1994.